

# An Optimal Multiquadric Variable Shape Parameter for Boundary Value Problems Using Particle Swarm Optimization

Abdoulhafar Halassi Bacar<sup>1</sup> & Said Charriffaini Rawhoudine<sup>1</sup>

<sup>1</sup> Univesité des Comores, Faculté des Sciences et Techniques, Département des Mathématiques, Physique et Chimie, Laboratoire des Mathématiques, Statistiques, Informatique et Applications (LMSIA), BP 2585 Moroni, Union des Comores

Correspondence: Said Charriffaini Rawhoudine, Univesité des Comores, Faculté des Sciences et Techniques, Département des Mathématiques, Physique et Chimie, Laboratoire des Mathématiques, Statistiques, Informatique et Applications (LMSIA), BP 2585 Moroni, Union des Comores. E-mail: crawhoudine@gmail.com

Received: December 4, 2023 Accepted: March 12, 2024 Online Published: May 2, 2024

doi:10.5539/jmr.v16n2p108 URL: <https://doi.org/10.5539/jmr.v16n2p108>

## Abstract

The multiquadric radial basis function method has been widely used to solve partial differential equations-based problems regarding its flexibility and meshfree characteristics. The accuracy and stability of this method are derived and based on the use of a free-shape parameter that sensibly controls the comportment of the technique. Significant improvements have already been reported and show that variable shape parameters conduct the method to handle problems with striking results compared to global-based techniques. Nevertheless, choosing a suitable set of shape parameters is still an open topic because of the complexity of the method when the number of collocation points increases. The current work proposes a variant particle swarm optimization based on local displacement with attractors to determine the multi-quadratic function's "best" optimal variable shape parameter in solving boundary value problems. Based on an initially random set of variable shape parameters, the proposed algorithm first performs and evaluates the errors between the expected exact solution and the approximate solution thoroughly. In the first stage, the particle swarm algorithm search for an optimal set of shape parameters that minimize the error and the conditioning number of the radial basis system matrix. In the second stage, the obtained optimal set of shape parameters is applied to solve the considered problem. In this way, when the number of collocation points increases, the first stage based on particle swarm optimization stabilizes the strategy. It proposes an "acceptable" set of shape parameters for the given problem. The proposed method is applied to a set of well-known boundary value problems in one and two-dimensional spaces and compared to other techniques published in the literature. The results show that the proposed method achieves more accurate solutions than recently proposed in the literature.

**Keywords:** multiquadric function, shape parameter, boundary value problems, particle swarm optimization, local attractors

## 1. Introduction

Boundary value problems are essential to numerical physics and mathematical modeling (Adewumi et al., 2020; Henderson & Luca, 2016). They occur in many applications such as wave propagation (Egorova & Ye 2020), electrostatics (Duan et al., 2013), deflection of cantilever beams under concentrated load, the temperature distribution of the radiation fin of the trapezoidal profile, and potential theory among other engineering applications. In general, the problem statement, in this class of problems, consists of mathematically solving the following boundary value problem:

$$\begin{cases} \mathcal{L}u(\mathbf{x}) = f(\mathbf{x}), & \mathbf{x} \in \Omega_I, \\ \mathcal{B}u(\mathbf{x}) = g(\mathbf{x}), & \mathbf{x} \in \Omega_B, \end{cases} \quad (1)$$

where  $\mathcal{L}$  and  $\mathcal{B}$  are sums of linear partial differential operators;  $\Omega = \Omega_I \cup \Omega_B$  is the entire domain where  $\Omega_I$  contains the  $N_I$  interior collocation points, and  $\Omega_B$  contains the  $N_B$  boundary points. For simplicity, we shall assume that the collocation points are arranged in a set  $S$  and the boundary points are classed at the end of the set so that:

$$S = \{1, \dots, N_I, N_I + 1, \dots, N\}, \quad (2)$$

where  $N = N_I + N_B$  is the total number of collocation points.

The most popular techniques used for spatial derivatives approximations are mesh-based techniques such as finite difference, finite element, or finite volume methods. These mesh-based techniques have been widely used in recent decades to

solve partial differential equations. However, the quality of meshes, stabilization techniques, and solutions to Riemann problems alter the accuracy of mesh-based techniques, which hinders their applications for solving real problems with irregular domains and complex Riemann problems. Stabilization techniques such as introducing artificial viscosity, flux limiters, and relaxation schemes are proposed. If the flux limiters techniques ensure high-order stabilized schemes, they are not adapted for complexly shaped domains.

For numerical methods, meshless techniques are significantly developed for solving linear and nonlinear partial differential equations. More extensive studies have been focused on meshless radial basis functions (RBF); their applications in partial differential equations provided favorable results. The multiquadric RBF was contrived and applied to scattered data interpolations, which required particular observations and optical research (Micchelli, 1986; Wendland, 2005). To illustrate, a typical example of the application of RBF methods for scattered data interpolation is studied in the articles (Buhmann, 2003; Kansa, 2009; Powell, 1992). The RBF applications provide solvability, convergence, and stability towards steady, time-dependent partial differential equations (PDE), and different PDEs problems (Golberg & Chen, 1994; Kansa et al., 2004). Furthermore, these solvers are based on a global formulation of meshless techniques governed by full differentiation matrices, for which a shape parameter controls the invertibility. While collocation points are refined, the choice of a suitable shape parameter becomes difficult; this may result in ill-conditioned matrices, and their invertibility becomes arduous. Solving partial differential problems using radial basis functions is suited to choosing an “optimal” shape parameter in its global formulation or an “optimal” set of shape parameters in the variable version. The problem is then conditioned to an optimization problem. Numerous strategies are proposed and used for the problems related to shape parameters. A global shape parameter has been proposed and used in many works (Hardy, 1971; Franke, 1979b; Fasshauer & Zhang, 2007). Later, variable shape parameters are introduced and applied to interpolation problems and partial differential problems (Kansa et al., 2009; Sarra & Sturgill, 2009; Xiang et al., 2012). Numerous works show that using variable shape parameter strategies is well-suited compared to the global shape parameter strategy (Fornberg & Zuev, 2007). Recent works have been developed to withstand new strategies on choosing optimal shape parameters radial basis functions based methods. In (Aiken et al., 2022; Zheng et al., 2020), an optimal shape parameter strategy is used on oscillatory radial basis function and least square approximation. While in (Skala et al., 2020; Yaghouti & Ramezannezhad Azarboni, 2017), estimation of shape parameters are used on radial basis formulation method. An optimal algorithm for choosing a good shape parameter in image processing is developed and application of optimal shape parameter on gaussian radial basis function is proposed in (Sun et al., 2023).

Optimization methods based on metaheuristics have been developed during the last decades. These are nature-inspired behavior algorithms that can search for an optimal or a set of optimal solutions for a complex optimization problem. For example, sea turtle foraging algorithms (STFA) are proposed in (Tansui & Thammano, 2016, 2020) for solving continuous optimization problems. The bond energy algorithm (BEA) was developed and used in the database design area to determine how to group and physically place data on a disk (Mehta et al., 2022). A combined local and global search algorithm is proposed in (Irfan Shirazi et al., 2023) for solving damage assessment in laminated composite plates. In contrast, in (Benaissa et al., 2021), the same algorithm is coupled with the POD-RBF technique for elastostatic and dynamic crack identification, and in (Khatir et al., 2023), authors proposed and hybrid PSO-YUKI for double cracks identification in CFRP cantilever beam. An application of the YUKI algorithm for experimental sensitivity analysis of sensor placement based on virtual springs and damage quantification and for optimal axial-probe design for Foucault-Current tomography is stated in (Slimani et al., 2022; Benaissa et al., 2023). Numerous variants of particle swarm optimization are proposed during these last years, and applications are underlined in vehicle routing problems using local displacement based on attractors (Halassi Bacar & Rawhoudine, 2021), continuous optimization problems using parallel global Best-Worst PSO algorithm (Kumar et al., 2023), optimization of convolutional neural networks architecture for image classification (Elhani et al., 2023).

Furthermore, metaheuristics are proposed in the same papers for searching for an optimal set of shape parameters on solving partial differential problems. In (Esmaeilbeigi & Hosseini, 2014), the genetic algorithm was used to find good shape parameters in interpolation problems and in Kansa's method for ordinary differential equations and partial differential equations using global shape parameters. A variable shape parameter version is proposed in (Afiatdoust & Esmaeilbeigi, 2015) on solving one-dimensional partial differential problems. Recent works have shown that particle swarm optimization strategies, initially proposed in (Kennedy & Eberhart, 1995), are compelling tools for optimization problems compared to evolutionary algorithms (Wang & Yang, 2010; Leung et al., 2014; Halassi, 2017). In (Koupaei et al., 2018), the native particle swarm optimization is adapted to find an optimal global shape parameter in solving PDEs.

The current work highlights the use of a PSO technique based on local displacement using a particle attractor for finding an optimal variable shape parameter. The main motivations consist of the reduced number of particles in the search space and the diversification tool of using local displacement during the search for optimum. It is well-known that native PSO-based algorithm converges quickly toward local optimum and can be retained in that region. Using local displacement

leads the particles to explore the entire search space and achieve the best approximation of a set of optimal variable shape parameters. Moreover, the results of MQ approximation are better where the shape parameter  $\varepsilon$  is small. At the same time, small  $\varepsilon$  produces ill-conditioned RBF matrices. Therefore, the singular value decomposition (SVD) is implemented as a regularization technique other than the standard linear solver (Tsai et al., 2010) and improves the accuracy of the PSO algorithm. The proposed algorithm is structured in two steps :

- The PSO algorithm based on local attractors is applied in a set of  $N$  collocation points to determine a set of  $N$  shape parameters ( $\varepsilon_i$ ) using the RMS error as the fitness function. That implies that each shape parameter  $\varepsilon_i$  generated is assigned to a collocation point  $\mathbf{x}_i$ .
- The optimal set of shape parameters is applied to Kansa's method to determine the approximation of the boundary value problem using the set of  $N$  collocation points used in the previous step.

To underline the accuracy and stability of the proposed algorithm, two one-dimensional boundary value problems are first solved using different strategies for fixing optimal shape parameters and compared with the obtained results using the proposed strategy in the current paper. Secondly, two-dimensional boundary value problems are solved in regular and irregular grids. Test problems are also considered in complexly shaped domains for which mesh-based methods are difficult to be applied. Based on the findings, it appears that the proposed method may offer greater accuracy and stability than other methods that have been previously studied and documented.

The paper follows a standard composition as follows. Kansa's radial basis function method is introduced and mathematically explained in Section 2. In Section 2, the adaptation of the particle swarm optimization algorithm for optimal variable shape parameters in Kansa's RBF method is outlined. The results and comments are presented in Section 3 and eventually Section 4, the conclusion of the proposed work.

## 2. Radial Basis Function Method

Let us consider the equation (1) that must be discretized with a set of  $N$  distinct points  $\mathbf{x} = \{\mathbf{x}_1, \dots, \mathbf{x}_N\}$  where  $\mathbf{x}_i \in \Omega \subset \mathbb{R}^2$  is called a center. The performance of mesh-free methods is that no restriction is imposed on the shape of the domain or on how the centers are generated. For a given collocation point  $\mathbf{x}_i$ , the meshfree method consists of an interpolation technique of the form

$$\hat{u}(\mathbf{x}_i) = \sum_{j=1}^N \lambda_j \phi(\|\mathbf{x}_i - \mathbf{x}_j\|_2, \varepsilon_i), \quad (3)$$

where  $\lambda = [\lambda_1, \dots, \lambda_N]^T$  is the expansion coefficient and  $\phi$  is a radial basis function. Conforming the principles of interpolation conditions

$$\hat{u}(\mathbf{x}_i) = u(\mathbf{x}_i), \quad \mathbf{x}_i \in \Omega, \quad (4)$$

give  $N$  linear equations generating an  $N \times N$  linear system

$$\mathcal{H}\lambda = u. \quad (5)$$

The interpolation matrix  $\mathcal{H}$  has the following elements

$$h_{ij} = \phi(\|\mathbf{x}_i - \mathbf{x}_j\|_2, \varepsilon_i), \quad 1 \leq i, j \leq N. \quad (6)$$

The solution  $\lambda$  of the equation (5) depends on the invertibility of the local system matrix  $\mathcal{H}$ . Here, we consider the multiquadric function defined by

$$\phi(r, \varepsilon) = \sqrt{1 + \varepsilon^2 r^2}, \quad (7)$$

with  $r = \|\mathbf{x} - \mathbf{x}_j\|_2$  is the Euclidean distance between the reference node and a supported neighbor within the collocation points and the shape parameter  $\varepsilon$  that controls the behavior of the interpolation matrix  $\mathcal{H}$ . If the invertibility of the matrix  $\mathcal{H}$  is assured, the expansion coefficient  $\lambda$  can be determined as

$$\lambda = \mathcal{H}^{-1}u. \quad (8)$$

To incorporate this scheme in the boundary value problem (1), derivatives of a function  $u$  at the center locations must be approximated. The linear differential operators  $\mathcal{L}$  and  $\mathcal{B}$  are applied to the equation (3) and evaluated at the centers

$$\begin{cases} \mathcal{L}\hat{u}(\mathbf{x}_i) = \sum_{j=1}^{N_I} \lambda_j \mathcal{L}\phi(\|\mathbf{x}_i - \mathbf{x}_j\|_2, \varepsilon_i), & \mathbf{x}_i \in \Omega_I, \\ \mathcal{B}\hat{u}(\mathbf{x}_i) = \sum_{j=N_I+1}^{N_B} \lambda_j \mathcal{B}\phi(\|\mathbf{x}_i - \mathbf{x}_j\|_2, \varepsilon_i), & \mathbf{x}_i \in \Omega_B, \end{cases} \quad (9)$$

And replaced them with the values referred to in equation (1), we obtain

$$\begin{cases} \sum_{j=1}^{N_I} \lambda_j \mathcal{L}\phi(\|\mathbf{x}_i - \mathbf{x}_j\|_2, \varepsilon_i) = f(\mathbf{x}_i), & \mathbf{x}_i \in \Omega_I, \\ \sum_{j=N_I+1}^{N_B} \lambda_j \mathcal{B}\phi(\|\mathbf{x}_i - \mathbf{x}_j\|_2, \varepsilon_i) = g(\mathbf{x}_i), & \mathbf{x}_i \in \Omega_B. \end{cases} \quad (10)$$

Equation (10) can be written more concisely as a matrix product

$$\mathcal{A}\lambda = \mathcal{F}, \quad (11)$$

where  $\lambda$  is the  $N$ -valued column vector of expansion coefficient,  $\mathcal{A}$  is an  $N \times N$  matrix defined by

$$\begin{cases} a_{ij} = \mathcal{L}\phi(\|\mathbf{x}_i - \mathbf{x}_j\|_2, \varepsilon_i), & \text{if } \mathbf{x}_i \in \Omega_I, \\ a_{ij} = \mathcal{B}\phi(\|\mathbf{x}_i - \mathbf{x}_j\|_2, \varepsilon_i), & \text{if } \mathbf{x}_i \in \Omega_B, \end{cases} \quad (12)$$

and  $\mathcal{F}$  is an  $N$ -valued vector, with the values  $\mathbf{F}$  for  $\mathbf{x}_i \in \Omega_I$  and  $\mathbf{G}$  for  $\mathbf{x}_i \in \Omega_B$ , defined by

$$\mathcal{F} = \begin{bmatrix} \mathbf{F} \\ \mathbf{G} \end{bmatrix}. \quad (13)$$

Using the expansion coefficient (equation 8), the linear system, expressed in equation (11), becomes

$$\mathcal{A}\mathcal{H}^{-1}\hat{u} = \mathcal{F}, \quad (14)$$

which removes the dependence of the RBF scheme on the expansion coefficient  $\lambda$  and the approximated solution of the boundary value problem (1) can be found by the inverse of matrices as

$$\hat{u} = \mathcal{H}\mathcal{A}^{-1}\mathcal{F}. \quad (15)$$

If we define the associated  $N \times N$  matrix weights  $\mathcal{D}$  by

$$\mathcal{D} = \mathcal{H}\mathcal{A}^{-1}, \quad (16)$$

the boundary value problem (1) is solved by simply multiplying the right-hand side of the problem by the associated weights. It should also be stressed that to solve the linear systems resulting from the RBF method, we use the SVD algorithm to overwhelm the ill-conditioned matrix sensibility.

For all problems involving matrix, solutions are existential through the invertibility of the matrix. RBF-based meshless solutions are prone to the invertibility of the RBF derivative matrix  $\mathcal{A}$ . Besides, It is proven in the paperwork (Micchelli, 1986) that the invertibility is assured under the circumstance of using a constant shape parameter. Although, this invertibility is revoked if and when the matrix  $\mathcal{A}$  is singular (Hon & Schaback, 2001). The shape parameter affects both the

accuracy and the stability of the method. Global shape parameters, in certain works (Fasshauer & Zhang, 2007; Franke, 1979b; Hardy, 1971), portrayed great outcomes under circumstances of reasonable collocation points. When the domain is refined, the global shape parameters produce ill-conditioned matrices, and accuracy and stability are no longer guaranteed. Recently, techniques have been proposed to improve the accuracy of the RBF method using variable shape parameters. The well-known shape parameter in math literature is the exponential shape parameter (Kansa et al., 2009), defined by

$$\varepsilon_i = \left[ \varepsilon_{\min}^2 \left( \frac{\varepsilon_{\max}^2}{\varepsilon_{\min}^2} \right)^{\frac{i-1}{N-1}} \right]^{1/2}, \quad i = 1, \dots, N. \quad (17)$$

The random shape parameter (Sarra & Sturgill, 2009) defined by

$$\varepsilon_i = \varepsilon_{\min} + (\varepsilon_{\max} - \varepsilon_{\min}) \times \text{rand}(), \quad (18)$$

where rand is the MATLAB function that returns uniformly distributed pseudo-random numbers on the unit interval, and the trigonometric shape parameter (Xiang et al., 2012) given by

$$\varepsilon_i = \varepsilon_{\min} + (\varepsilon_{\max} - \varepsilon_{\min}) \times \sin(i), \quad (19)$$

where  $\varepsilon_{\min} = \frac{\sqrt{N}}{3}$  and  $\varepsilon_{\max} = \sqrt{N}$ , and  $N$  is the total number of nodes in one-dimensional approximations and is the node number of a row or a column in two-dimensional approximations. This interval is fixed empirically and can become unappropriated in a specific problem. In (Biazar & Hosami, 2016), the authors proposed an algorithm to find an appropriate interval for the shape parameter and apply one of the above variable shape parameters. Genetic algorithms are adapted in (Afiatdoust & Esmailbeigi, 2015) to find optimal variable shape parameters for one-dimensional boundary value problems. In the current work, a heuristic optimization method based on particle swarm strategies is proposed to fix variable shape parameters for Kansa's multiquadric method in one- and two-dimensional boundary value problems. The proposed strategy is detailed in the next Section.

Particle Swarm Optimization is classified as a global search heuristic based on population behavior. It is initially introduced for solving optimization problems (Eberhart & Kennedy, 1995) when searching for how to model social interactions between particles that must reach a given objective. The main population behavior description would be the fish school or bird flock searching for food or avoiding an obstacle. For shape parameter optimization, the initial population of particles is generated randomly in the range  $\varepsilon_{\min}$  and  $\varepsilon_{\max}$ . Each particle is represented by  $N$  coordinates respecting the  $N$  collocation points of Kansa's problem. At each iteration, each particle (shape parameter) moves towards the optimal shape parameter to minimize the numerical error of the desired problem. This movement is allowed by updating the position and the velocity of the particle following the best solution it has achieved so far and the global best solution of the whole swarm.

To introduce, let us consider a swarm of  $K$  particles representing  $K$  sets of shape parameters, where each particle is composed of a position

$$X_k = (X_{k1}, \dots, X_{kN}) \in \mathcal{X}, \quad (20)$$

where  $\mathcal{X}$  is the feasible space and velocity vector

$$V_k = (V_{k1}, \dots, V_{kN}). \quad (21)$$

Particles update their exploration directions using the following equations:

$$V_{k,i}^{(t+1)} = \omega V_{k,i}^{(t)} + c_1 r_1 (P_{k,i}^{(t)} - X_{k,i}^{(t)}) + c_2 r_2 (G_{b,i}^{(t)} - X_{k,i}^{(t)}), \quad (22)$$

$$X_{k,i}^{(t+1)} = X_{k,i}^{(t)} + V_{k,i}^{(t+1)}, \quad i = 1, \dots, N, \quad (23)$$

where  $\omega$  is the inertia factor that influences the local and global abilities of the algorithm,  $V_{k,i}^{(t)}$  and  $X_{k,i}^{(t)}$  are the  $i^{th}$  components of the velocity and the position of the particle  $k$  at iteration step  $t$ . The parameters  $c_1$  and  $c_2$  are weights affecting the cognitive and social factors, respectively, while  $r_1$  and  $r_2 \sim \mathcal{U}(0, 1)$  are randomly chosen at each stage.  $P_{k,i}^{(t)}$  stands for

the  $i^{th}$  component of the best value found by particle  $k$  (pBest) until the iteration  $t$  and  $G_{b,i}^{(t)}$  denotes the  $i^{th}$  component of the global best found by the entire swarm (gBest) till there. The equations (22) and (23), the personal best and global best positions, are used for updating particle velocity and position.

During the computation process of the particles in the classic PSO when solving constrained optimization problems, it is also possible that the particles move outside of the search space. It is therefore recommended to limit the search space by relocating the particles, i.e., replacing position values of the particles between a minimum and a maximum value. In the current work, to avoid the empirical determination of  $\varepsilon_{\min}$  and  $\varepsilon_{\max}$ , we consider that the search space is opened, and shape parameters can take any real value if this can improve the approximation solution. Negative shape parameter values are authorized since they do not affect the final procedure in Kansa's method; they are exploited as square numbers (equation 7).

### 2.1 Local Displacement Using Attractors

Instead of using the basic displacement as described in equations (22)-(23), we incorporate another displacement based on the local attraction of particles. The idea is that a given particle at the position  $X_k^{(t)}$ , when knowing its best personal performance  $P_k^{(t)}$  and the best global performance  $G_b^{(t)}$  of the swarm, moves around intermediate local positions before reaching its new position  $X_k^{(t+1)}$ . If we note  $S_k^{(t)}$  and  $T_k^{(t)}$ , these local intermediate positions, the classical and the new proposed displacements, are illustrated in Figure 1.

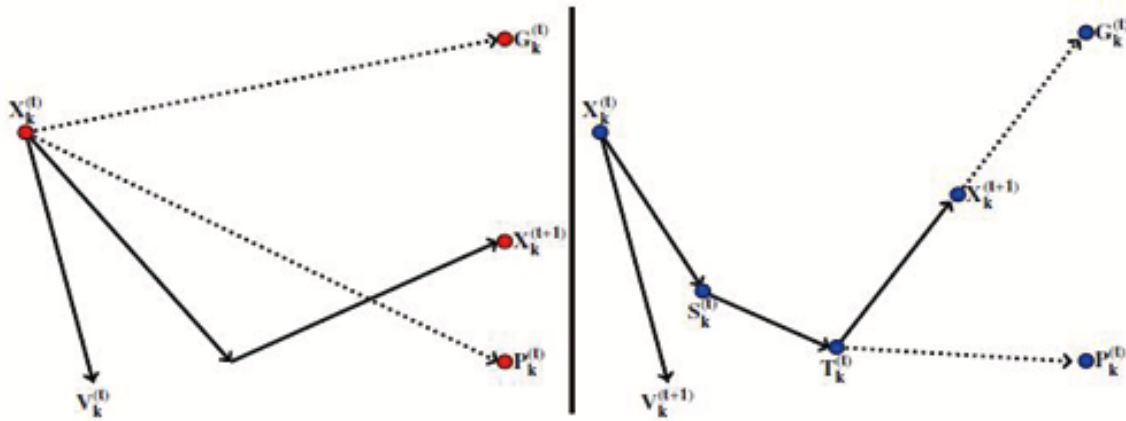


Figure 1. Particle displacement mechanism at each iteration in the native PSO version (left) and when using local attractors (right)

With this displacement mechanism, at each iteration step  $t$ , two intermediate positions  $S_k^{(t)}$  and  $T_k^{(t)}$  are reached by the particle before attending its final position  $X_k^{(t+1)}$ . All the components of the new particle position and velocity are determined by following four equations (Halassi, 2017):

$$\begin{aligned} S_{k,i}^{(t)} &= X_{k,i}^{(t)} + c_1 V_{k,i}^{(t)}, \\ T_{k,i}^{(t)} &= S_{k,i}^{(t)} + c_2 r_2 (P_{k,i}^{(t)} - S_{k,i}^{(t)}), \\ X_{k,i}^{(t+1)} &= T_{k,i}^{(t)} + c_3 r_3 (G_{b,i}^{(t)} - X_{k,i}^{(t)}), \\ V_{k,i}^{(t+1)} &= \alpha V_{k,i}^{(t)} + \beta (P_{k,i}^{(t)} - X_{k,i}^{(t)}) + \gamma (G_{b,i}^{(t)} - X_{k,i}^{(t)}), \end{aligned} \quad (24)$$

where

$$\alpha = c_1(1 - c_2 r_2) \times (1 - c_3 r_3), \quad \beta = c_2 r_2(1 - c_3 r_3), \quad \text{and} \quad \gamma = c_3 r_3. \quad (25)$$

$c_1$ ,  $c_2$ , and  $c_3$  are given parameters;  $r_1$ ,  $r_2$ , and  $r_3 \sim \mathcal{U}(0, 1)$  are randomly variable parameters. To ensure convergence of the approach, parameters  $c_1$ ,  $c_2$ , and  $c_3$  must be taken according to one of the following two sets (Tchomté & Gourgand, 2009; Halassi, 2017) :

$$0 < c_1 < 0.9; \quad 0 < c_2 < 2; \quad 0 < c_3 < 2, \quad (26)$$

$$0 < c_1 < 0.9; \quad 2 \leq c_2 < 4; \quad 2 \leq c_3 < 4. \quad (27)$$

## 2.2 Fitness Function

The main idea of this paper is to determine an optimal set of shape parameters that minimizes the computation of the residual error in the collocation points. Therefore, the Root Mean Square (RMS) error is considered in both subsets, interior, and boundary points. Let us recall that the native RMS error is defined by

$$R = \sqrt{\frac{\sum_{i=1}^N (u(\mathbf{x}_i) - \hat{u}(\mathbf{x}_i))^2}{N}}, \quad (28)$$

where  $u(\mathbf{x}_i)$  and  $\hat{u}(\mathbf{x}_i)$  are the exact and numerical solutions at the collocation point  $\mathbf{x}_i$ . The fitness function  $R$  is a summation of RMS error in the interior and boundary test points. However, the exact solution to a problem could be unknown in the select interval. In this regard, the optimization problem can be reformulated as a minimization of the fitness function concerning the particle  $\varepsilon$  formed by the RMS error. For a given set of shape parameters  $\varepsilon = \{\varepsilon_1, \dots, \varepsilon_N\}$ , the cost function of optimization problem is:

$$\min_{\varepsilon \in \mathbb{R}^N} R(\varepsilon) = \sqrt{\frac{\sum_{i=1}^{N_I} (\mathcal{L}\hat{u}(\mathbf{x}_i, \varepsilon_i) - f(\mathbf{x}_i))^2}{N_I}} + \sqrt{\frac{\sum_{i=N_I+1}^N (\mathcal{B}\hat{u}(\mathbf{x}_i, \varepsilon_i) - g(\mathbf{x}_i))^2}{N_B}} \quad (29)$$

where  $\hat{u}(\mathbf{x}_i, \varepsilon_i)$  denote the approximate solution at the test point  $\mathbf{x}_i$  using a variable shape parameter  $\varepsilon_i$ .

## 3. Numerical Results

The algorithm is performed on the Mathworks® MATLAB R2017b on a PC which has the current specifications: Intel® Core™ i7-7700HQ CPU @2.80GHz, CUDA cores 1280 NVIDIA GeForce GTX 1060, and 8GB RAM. The operation system is Windows 10 pro.

To demonstrate the effectiveness and stability of the population-based method proposed in the last section, a set of examples of partial differential equations in 1D and 2D spaces are presented in this section, respectively. The RMS error is integrated into the PSO strategy for selecting the optimal shape parameters; consequently, it is then used to compare the proposed technique to other selected techniques in the literature. In this section, we consider the Finite Difference scheme noted (FD), the RBF scheme using a global shape parameter without particle swarm optimization (GRBF), the RBF scheme using variable shape parameters without particle swarm optimization (VRBF), and the RBF scheme using global shape parameter with particle swarm optimization (GRBF-PSO) and the variable shape parameter with particle swarm optimization (VRBF-PSO).

### 3.1 One-dimensional Test Problems

To compare the proposed strategy to those from the literature, we choose two one-dimensional boundary value problems solved in recent papers. In both examples, the inertia weight is set to be  $\omega = 1$  while the other parameters are taken as  $c_1 = 0.5$ ,  $c_2 = 3.7$ , and  $c_3 = 2.25$ . The number of iterations is taken  $T = 50$ ,  $N$  the number of collocations points, and the population size of the shape parameter is set  $K = 20$ .

#### 3.1.1 Dirichlet Boundary Conditions

The first test problem considered below is a one-dimensional boundary-valued problem with Dirichlet boundary conditions as

$$\begin{aligned} \frac{\partial}{\partial x} u(x) + u(x) &= f(x), \quad x \in \Omega, \\ u(x) &= g(x), \quad x \in \partial\Omega, \end{aligned} \quad (30)$$

where  $\Omega = [0.5, 1.5]$  and the functions  $f(x)$  and  $g(x)$  are taken according to the exact solution

$$u(x) = \frac{1}{1 + 4(x - 1)^2}. \quad (31)$$

This problem is solved in (Afiatdoust & Esmailbeigi, 2015) using genetic algorithms for choosing optimal variable shape parameters, and obtained results are compared with those from other strategies for variable shape parameters. In this paper, we compare obtained results with those from global strategies with or without the PSO algorithm and those from variable strategies without PSO techniques. In the variable strategy without PSO, we use the random shape parameter (equation 18) while in the global strategy of an optimal shape parameter without PSO, we use the Franke proposition (Franke, 1979a) which consists of taking

$$\varepsilon = \frac{\sqrt{N}}{1.25D}, \quad (32)$$

where  $N$  is the number of collocation points and  $D$  is the diameter of the smallest centered circle that contains all the collocation points. RMS errors and CPU times of the obtained results are summarized in Table 1.

Table 1. RMS Errors and CPU times for the problem (30) using different sets of collocation points and different strategies to choose the optimal shape parameters

| N    |           | FD         | GRBF        | VRBF       | GRBF-PSO   | VRBF-PSO   |
|------|-----------|------------|-------------|------------|------------|------------|
| 50   | RMS error | 5.4707E-03 | 8.8997E-06  | 2.9070E-09 | 2.9105E-09 | 1.4229E-09 |
|      | CPU time  | 0.015625   | 0.015625    | 0.031250   | 2.7500     | 2.2656     |
| 100  | RMS error | 2.8241E-03 | 3.71556E-07 | 2.6762E-12 | 6.8739E-10 | 1.3547E-14 |
|      | CPU time  | 0.031250   | 0.046875    | 0.015625   | 9.7813     | 8.0781     |
| 200  | RMS error | 1.4340E-03 | 1.5823E-08  | 1.9504E-15 | 9.2898E-10 | 1.3909E-15 |
|      | CPU time  | 0.015625   | 0.234380    | 0.140630   | 25.9840    | 27.8590    |
| 400  | RMS error | 7.2245E-04 | 5.3488E-08  | 5.3330E-15 | 1.8171E-09 | 1.5252E-15 |
|      | CPU time  | 0.015625   | 0.281250    | 0.265630   | 135.2200   | 143.7300   |
| 800  | RMS error | 3.6259E-04 | 1.4263E-07  | 5.7205E-15 | 2.8323E-09 | 1.6772E-15 |
|      | CPU time  | 0.078125   | 0.781250    | 0.7500     | 573.8900   | 622.8000   |
| 1600 | RMS error | 1.8163E-04 | 2.8204E-07  | 2.5855E-14 | 3.2236E-09 | 2.0667E-15 |
|      | CPU time  | 1.0938     | 3.4844      | 3.4688     | 872.0000   | 954.3000   |

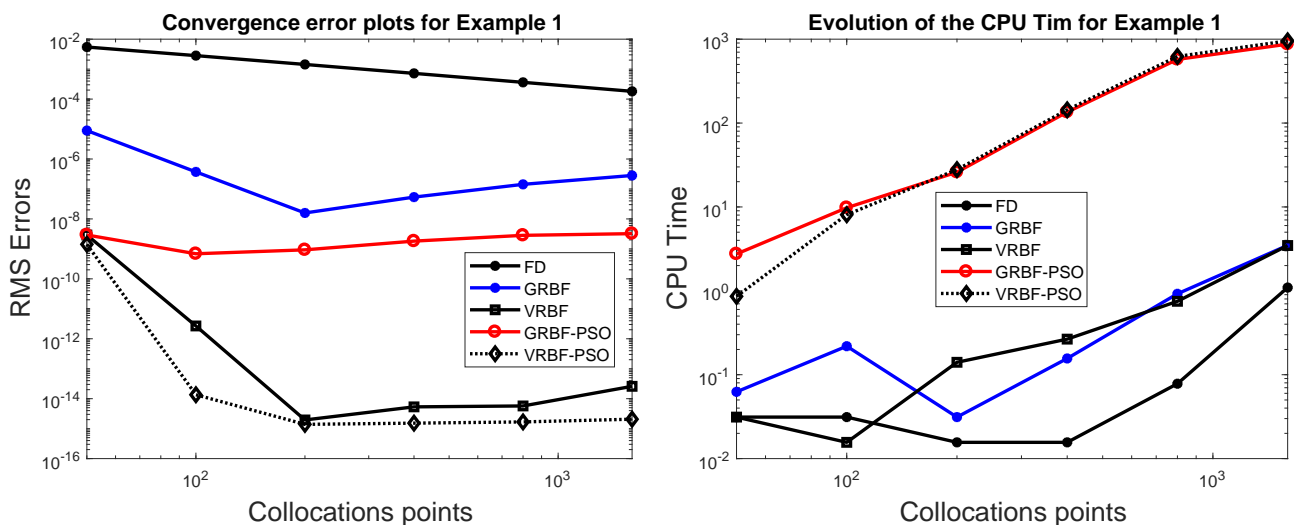


Figure 2. Convergence plots (for the problem (30)) comparison of the selected methods : Evolution of the error (left) and the conditioning number (right)

In Table 1, we depict the RMS errors and the CPU time for the FD scheme, the GRBF, the VRBF, the GRBF-PSO, and the VRBF-PSO. Results show that obtained results using the PSO technique to choose a global shape parameter are worse



than those with variable strategy without the PSO technique. Using the PSO technique on a variable strategy of setting the MQ shape parameters can improve the approximated solution. The PSO strategy of selecting variable shape parameters gives interesting results in all the selected techniques. Even though the RMS errors are insignificant, the drawback of this strategy is the highest CPU time. In Figure (2), the RMS errors and the CPU times are plotted according to the number of collocation points. It is clear that the PSO-based strategy on variable shape parameters gives interesting results regarding errors and convergence. Nevertheless, the strategy needs more CPU time because of the two-stage strategies. The PSO-based technique is interesting while the number of collocation points increases. This predictor strategy allows the method to fix a suitable set of shape parameters. The sensibility of the RBF matrices using the different strategies for optimal shape parameters is depicted in Table 2 as follows: optimal shape parameters and the corresponding condition numbers of the matrices for the MQ-based schemes according to the collocation points. Especially the variable shape parameter strategy is represented by the mean value of the optimal set of shape parameters, and in the PSO-based strategies, the absolute values are considered. Results show that using the PSO technique on variable optimal shape parameters leads the RBF algorithm to take optimal values in a large range of values. Many possibilities are offered, and they lead the condition number to remain in the same interval as when the other strategies are applied. This wide possible choice of selecting the optimal set of shape parameters may be the reason that the associated RMS error remains very small. Obtained numerical results for the strategies based on PSO techniques are depicted in Figure 3, where the number of collocation points is  $N = 50$  and  $N = 100$ .

Table 2. Mean of the optimal shape parameters, and associated condition numbers for the problem (30) using different sets of collocation points for the different optimal shape parameters strategies

| N    |              | GRBF      | VRBF        | GRBF-PSO    | VRBF-PSO    |
|------|--------------|-----------|-------------|-------------|-------------|
| 50   | Mean shape   | 5.6568    | 4.5768      | 2.2624      | 16.1920     |
|      | Cond. number | 5.0036E12 | 9.4456E16   | 1.4425E18   | 1.0339E09   |
| 100  | Mean shape   | 8.0000    | 6.6875      | 1.5700      | 8.4188      |
|      | Cond. number | 1.1097E18 | 5.1716E18   | 1.2121E19   | 8.5911E18   |
| 200  | Mean shape   | 11.3137   | 9.4614      | 1.546       | 16.744      |
|      | Cond. number | 5.8632E18 | 7.8326E18   | 4.1575E19   | 6.4619E19   |
| 400  | Mean shape   | 16.0000   | 13.3860     | 1.8278      | 6.4124      |
|      | Cond. number | 6.1740E19 | 2.0313E19   | 4.3567E20   | 3.0164E20   |
| 800  | Mean shape   | 22.6274   | 18.781      | 1.599       | 31.597      |
|      | Cond. number | 6.9091E19 | 1.2528E20   | 3.5081E20   | 8.2772E20   |
| 1600 | Mean shape   | 3.0000    | 26.8250     | 1.5728      | 13.0590     |
|      | Cond. number | 1.0111E21 | 1.760500E20 | 3.353600E22 | 8.004200E20 |

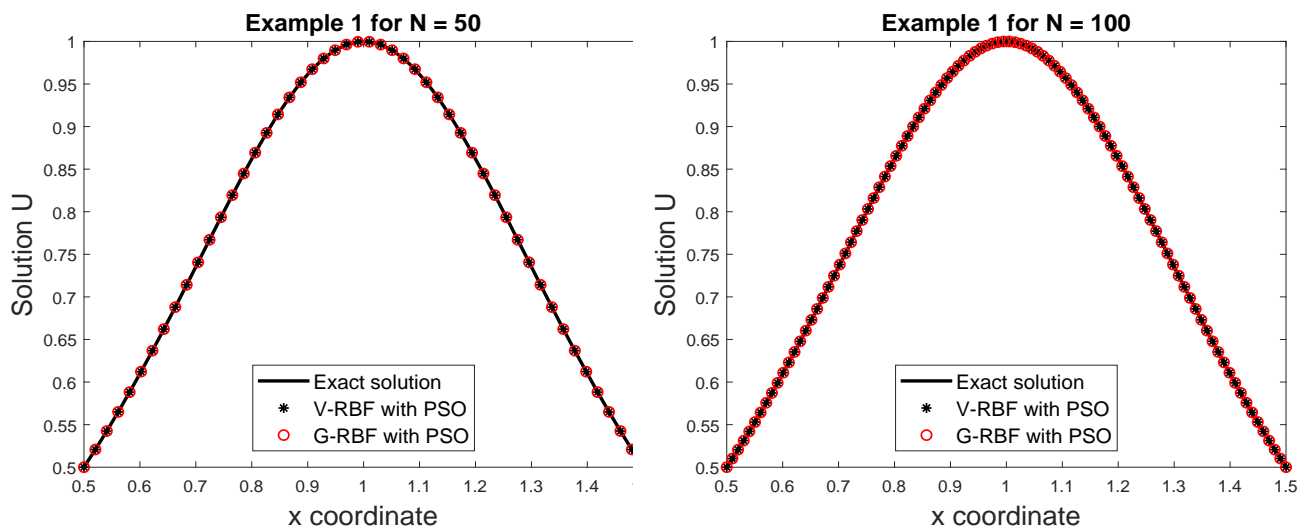


Figure 3. Numerical results (for the problem (30)) obtained in variable and global strategies in PSO technique using 50 collocation points (left) and 100 collocation points (right)

### 3.1.2 Periodic Boundary Conditions

Next, we consider the two-point second order one-dimensional boundary value problem (Siraj-ul-Islam, 2010) defined by

$$\frac{\partial^2}{\partial x^2} u(x) - u(x) = f(x), \quad x \in ]0; 1[, \quad (33)$$

subject to the periodic boundary conditions

$$u(0) = u(1), \quad u'(0) = u'(1). \quad (34)$$

The second member  $f(x)$  and the exact solution associated with this problem are defined respectively by

$$f(x) = -\sin(2\pi x) \left(1 + 4\pi^2\right) \left(x^3 - \frac{4}{3}x^2 + \frac{x}{3}\right) + \left(6x - \frac{8}{3}x\right) \sin(2\pi x) + 4\pi \cos(2\pi x) \left(3x^2 - \frac{8}{3}x + \frac{1}{3}\right), \quad (35)$$

and

$$u(x) = \sin(2\pi x) \left(x^3 - \frac{4}{3}x^2 + \frac{x}{3}\right). \quad (36)$$

Once again, we compare obtained results with those from global strategies with or without the PSO algorithm and those from variable strategies without PSO techniques. We use the same strategies as in the first example for the optimal shape parameters without the PSO algorithm. The results' computed RMS errors and CPU times are summarized in Table 3.

Table 3. RMS Errors and CPU times for the problem (33) using different sets of collocation points and different strategies to choose the optimal shape parameters

| N    |           | FD           | GRBF         | VRBF         | GRBF-PSO     | VRBF-PSO     |
|------|-----------|--------------|--------------|--------------|--------------|--------------|
| 50   | RMS error | 1.1785E-03   | 5.2418E-06   | 3.5812E-09   | 3.9722E-08   | 1.5257E-09   |
|      | CPU time  | 0.0156       | 0.5469       | 0.1406       | 2.8438       | 2.9844       |
| 100  | RMS error | 6.4382E-04   | 1.0247E-07   | 7.2014E-12   | 1.1219E-08   | 1.6329E-12   |
|      | CPU time  | 0.0313       | 0.0313       | 0.0156       | 7.8438       | 8.0156       |
| 200  | RMS error | 3.3579E-04   | 3.7257E-07   | 1.2467E-13   | 7.4804E-09   | 1.0056E-14   |
|      | CPU time  | 0.0312       | 0.0625       | 0.2031       | 28.3910      | 28.5780      |
| 400  | RMS error | 1.7139E-04   | 6.6991E-07   | 1.4939E-13   | 9.7445E-10   | 5.9575E-15   |
|      | CPU time  | 0.0469       | 0.2031       | 0.2188       | 136.9400     | 152.8400     |
| 800  | RMS error | 8.6572E-05   | 4.5573E-07   | 6.1658E-14   | 9.9839E-10   | 5.6552E-15   |
|      | CPU time  | 0.0625       | 0.6875       | 0.8281       | 597.6100     | 649.1700     |
| 1600 | RMS error | 4.350600E-05 | 3.091400E-06 | 7.493200E-14 | 2.039300E-10 | 8.506400E-15 |
|      | CPU time  | 0.328130     | 1.281300     | 1.500000     | 888.8100     | 960.6600     |

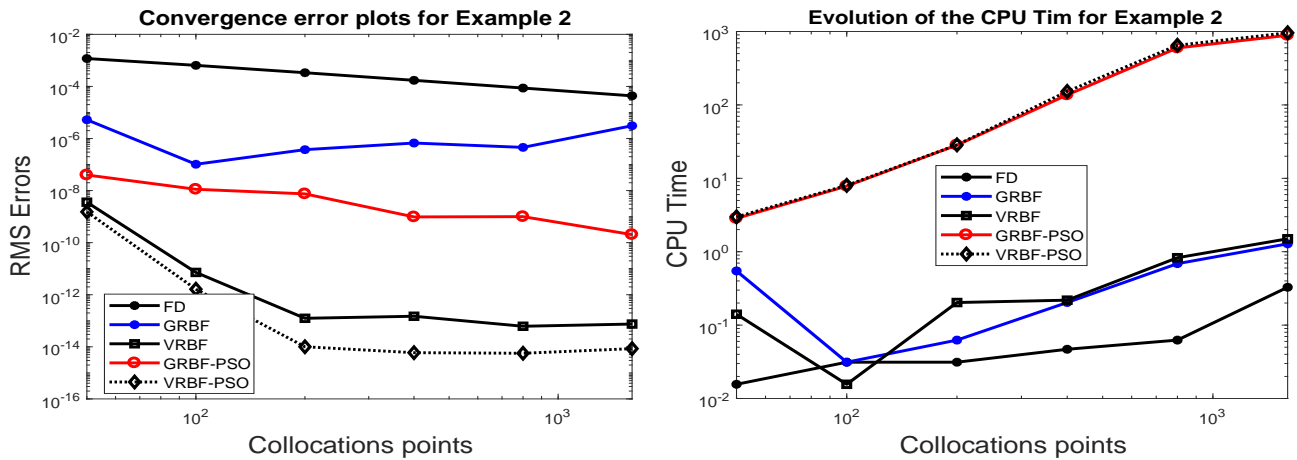


Figure 4. Convergence plots (problem (33)) comparison of the selected methods : Evolution of the error (left) and the conditioning number (right)

Results from Table 3 underline once more that searching an optimal set of variable shape parameters in the MQ-meshfree method gives more accurate numerical solutions in one-dimensional boundary value problems. The RMS errors remain close to zero even though the CPU time is important. Figure (4) plots the convergence curves and the CPU time evolution for the different numerical schemes considered. From depicted results, one can remark that solutions from variable shape parameter strategies are more accurate than those from other schemes. Moreover, the variable shape parameter strategy based on particle swarm optimization gives more important results according to convergence and stability. Once more, this strategy needs high CPU time because of the considered two stages (shape parameter optimization and numerical solution computation). The sensibility of the invertibility of the RBF matrices when using different strategies for optimal shape parameters is outlined in Table 4, where the final optimal shape parameters and the corresponding condition numbers of the RBF matrices are presented. We take the mean value of the optimal set of shape parameters for the variable shape parameters strategies, and for PSO-based strategies, the absolute values are considered. Results show that using the PSO technique on variable and global optimal shape parameters leads the RBF algorithm to take optimal values in a large range of values. Many possibilities are offered leading the condition number to remain in the same interval as the other strategies. In the PSO variable shape parameter case, the condition number becomes greater than the condition number from other strategies, in order of  $10^{20}$ , without affecting the invertibility of the matrix sensibly. In Figure 5, obtained numerical results for the strategies based on PSO techniques are depicted where the number of collocation points is  $N = 50$  and  $N = 100$ .

Table 4. Mean of the optimal shape parameters and associated condition numbers for the problem (33) using different sets of collocation points for the different optimal shape parameters strategies

| N    |              | GRBF        | VRBF        | GRBF-PSO    | VRBF-PSO    |
|------|--------------|-------------|-------------|-------------|-------------|
| 50   | Mean shape   | 5.6569      | 5.0257      | 2.4683      | 5.0339      |
|      | Cond. number | 2.9534E10   | 2.5401E14   | 3.7177E17   | 2.3132E17   |
| 100  | Mean shape   | 8.0000      | 6.4679      | 6.5979      | 14.3070     |
|      | Cond. number | 3.7771E15   | 4.1590E18   | 7.7525E17   | 1.3708E16   |
| 200  | Mean shape   | 11.3140     | 9.3671      | 13.9960     | 14.2510     |
|      | Cond. number | 9.2451E18   | 7.2086E18   | 4.4241E17   | 7.7424E18   |
| 400  | Mean shape   | 16.0000     | 13.2380     | 29.5120     | 21.5420     |
|      | Cond. number | 1.4378E19   | 6.2936E19   | 1.2557E18   | 4.3453E20   |
| 800  | Mean shape   | 22.6270     | 18.8360     | 62.2570     | 38.2580     |
|      | Cond. number | 5.0793E19   | 9.6362E19   | 6.6778E17   | 4.1678E20   |
| 1600 | Mean shape   | 32.0000     | 26.5980     | 119.7100    | 89.4610     |
|      | Cond. number | 4.079700E21 | 8.852600E19 | 3.066900E17 | 7.947600E21 |

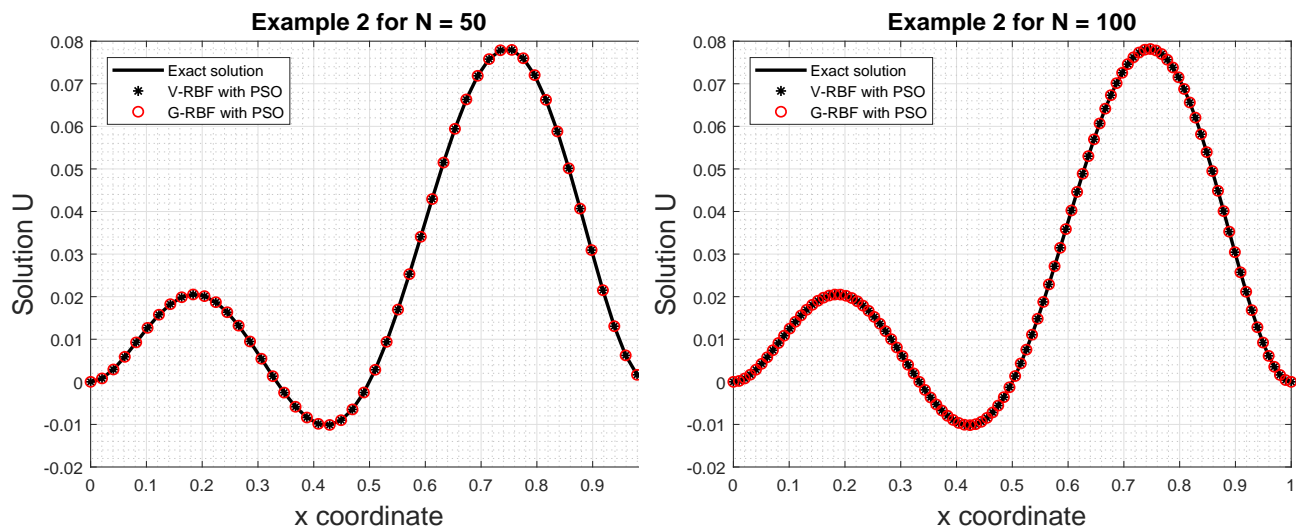


Figure 5. Numerical results (for the problem (33)) obtained in variable and global strategies in PSO technique using 50 collocation points (left) and 100 collocation points (right)

### 3.2 Two-dimensional Test Problems

As in the one-dimensional case, the shape parameter in the global strategy without PSO is fixed according to (Franke, 1979a), and the variable shape parameter is taken from the random shape parameter (18) in (Sarra & Sturgill, 2009) in all our computations. In all the following numerical simulations, the PSO parameters are fixed to be  $\omega = 0.75$ ,  $c_1 = 0.68$ ,  $c_2 = 1.25$ , and  $c_3 = 1.25$ . We examine the performance of our optimal shape parameter strategy for the following well-known two-dimensional boundary value examples.

#### 3.2.1 Poisson Problem With Dirichlet Boundary Conditions

Consider the two-dimensional Poisson problem as follows:

$$\begin{aligned} \nabla^2 u(x, y) &= f(x, y), \quad (x, y) \in \Omega, \\ u(x, y) &= g(x, y), \quad (x, y) \in \partial\Omega \end{aligned} \quad (37)$$

where  $\Omega = [0, 1] \times [0, 1]$  and the functions  $g(x, y)$  and  $f(x, y)$  are taken according to the exact solution

$$u(x, y) = \exp\left((x - 0.5)^2 - 0.5(y - 0.5)^2\right). \quad (38)$$

Table 5. RMS errors, CPU times, and mean of the optimal shape parameters for Example (problem (37)) using different numbers of population size in the swarm

| K  | 20 × 20 collocation points |          |        | 40 × 40 collocation points |          |         |
|----|----------------------------|----------|--------|----------------------------|----------|---------|
|    | RMS error                  | CPU time | Shape  | RMS error                  | CPU time | Shape   |
| 5  | 4.6196E-07                 | 25.7660  | 5.2900 | 8.5769E-10                 | 486.9700 | 8.8016  |
| 10 | 4.2071E-06                 | 52.1250  | 7.9133 | 4.6557E-09                 | 956.2500 | 14.6000 |
| 20 | 3.1334E-07                 | 102.3600 | 1.3120 | 1.1027E-09                 | 1906.500 | 24.3470 |

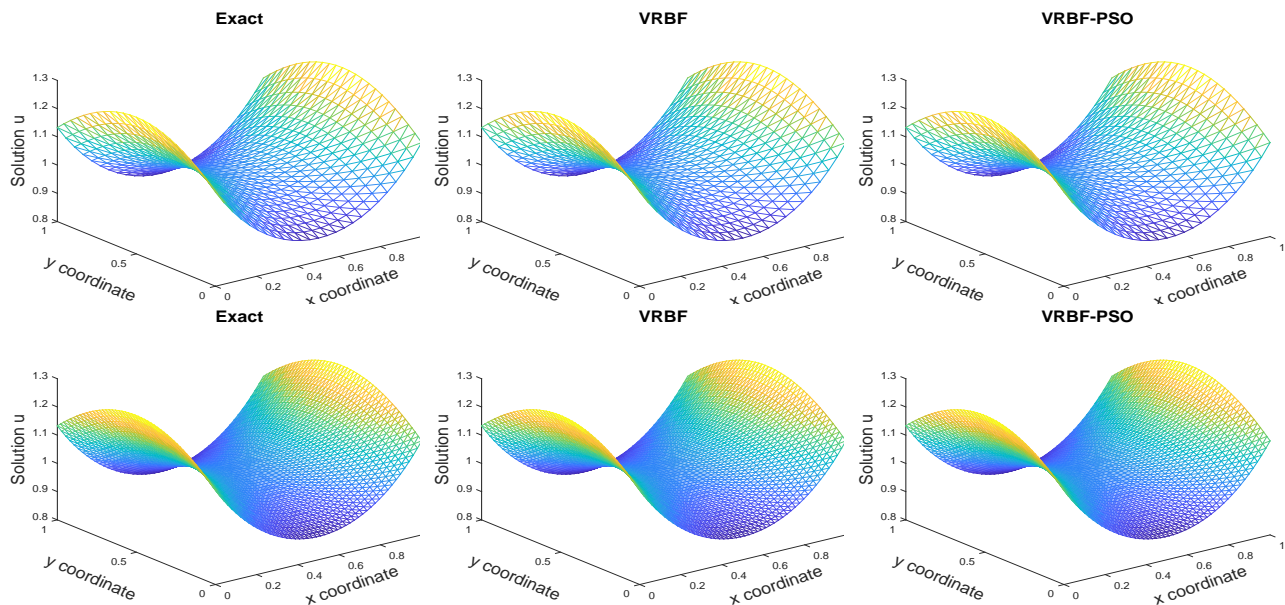


Figure 6. Results for the problem (37) in  $25 \times 25$  gridpoints (first line) and  $50 \times 50$  gridpoints (second line) using the exact solution (first column), VRBF strategy (second column), and VRBF-PSO strategy (third column)

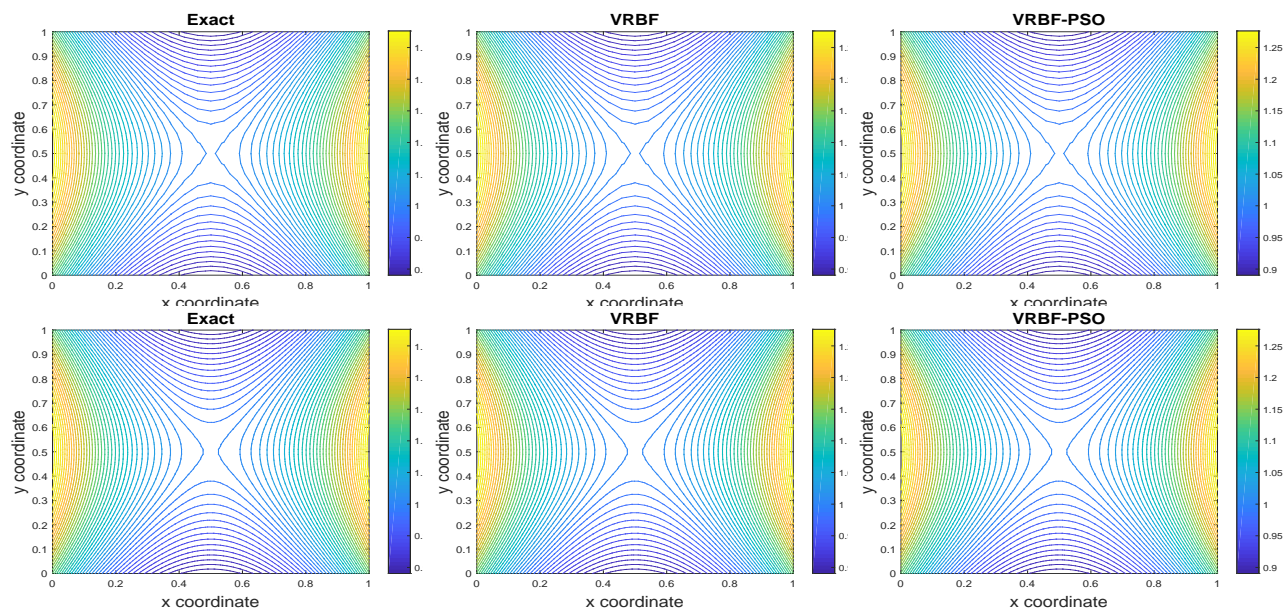


Figure 7. Contourlines for the problem (37) in  $25 \times 25$  gridpoints (first line) and  $50 \times 50$  gridpoints (second line) using the exact solution (first column), VRBF strategy (second column), and VRBF-PSO strategy (third column)

In the first step, we want to study how sensitive is the proposed strategy when varying the swarm's population size. Hence, we solve the problem (37) in uniformly distributed collocation points in the square  $[0; 1] \times [0; 1]$  using two sets of collocation points,  $20 \times 20$  collocation points and  $40 \times 40$  collocation points, by varying the number of the swarm size in the PSO procedure. The number of iterations is fixed to be  $T = 20$ . Table 5 presents RMS errors, CPU times, and the optimal set of shape parameters' mean value for  $K = \{5; 10; 20\}$  using the two sets of collocation points. From the results, we can observe that the number of particles in the swarm population does not sensibly affect the accuracy of the problem. The RMS error remains approximately the same. In contrast, this affects the CPU time considerably. Table 5 indicates that the CPU time is also doubled when the population size is doubled in the swarm. For that purpose, in all the following test problems, the swarm size will be stationary to  $K = 5$ .

Now, we solve the same problem (37) using different strategies for selecting optimal shape parameters in  $25 \times 25$  and  $50 \times 50$  collocation points. Figure 6 displays the computed numerical results using the PSO strategy in  $25 \times 25$  and  $50 \times 50$  collocation points. In Figure 7, we present the associated 50 equidistributed contour plots of these solutions. For comparisons, we have also included in these figures the obtained computational results using the analytical solutions and the approximated solutions using the variable shape parameter strategy without the PSO algorithm. For further numerical comparisons, we summarize, in Table 6, RMS errors, conditioning numbers, and optimal shape parameters for GRBF, VRBF, and VRBF-PSO strategies in the two sets of collocation points. Comparing the obtained results using the considered methods, it is clear that the presented strategy method produces accurate solutions for the considered problem. Our strategy method accurately approximates the numerical solution to this boundary value problem. The results shown below are favorable to the obtained results using other strategies.

Table 6. RMS errors, condition numbers, and mean of the optimal shape parameters for the Poisson example using different optimal shape parameters strategies

| N    |               | GRBF       | VRBF       | VRBF-PSO     |
|------|---------------|------------|------------|--------------|
| 625  | RMS error     | 6.1163E-06 | 6.2496E-08 | 8.199200e-07 |
|      | Cond. number  | 3.9967E17  | 7.00950E18 | 6.527600E16  |
|      | optimal shape | 2.828400   | 3.323600   | 18.625000    |
| 2500 | RMS error     | 5.0893E-07 | 5.2858E-10 | 4.8833E-11   |
|      | Cond. number  | 2.7535E20  | 6.5199E20  | 3.5284E20    |
|      | optimal shape | 4.000000   | 4.709200   | 22.754000    |

### 3.2.2 The Helmholtz Equation

Next, we consider the two-dimensional Helmholtz equation with Dirichlet boundary condition defined in (Tsai et al., 2010) by

$$\begin{aligned}\nabla^2 u(x, y) - u(x, y) &= f(x, y), \quad (x, y) \in \Omega, \\ u(x, y) &= g(x, y), \quad (x, y) \in \partial\Omega,\end{aligned}\quad (39)$$

where the domain  $\Omega$  is bounded with the Cassini curve defined by the parametric equation

$$\partial\Omega = \{(x, y) \in \mathbb{R}^2 : x = \rho \cos(\theta), y = \rho \sin(\theta), -\pi \leq \theta \leq \pi\}, \quad (40)$$

where

$$\rho = \left( \cos(3\theta) + \sqrt{2 - \sin^2(3\theta)} \right)^{1/3}. \quad (41)$$

The second member  $f$  is defined by

$$f(x, y) = -(1 + \pi^2)(x \sin(\pi y) + y \sin(\pi x)), \quad (42)$$

and  $g$  is defined according to the analytical solution

$$u(x, y) = y \sin(\pi x) + x \sin(\pi y). \quad (43)$$

We consider here the sets of collocation points depicted in Figure 8. The first set contains 110 boundary points and 731 interior points, while the second set is more refined with 167 boundary points and 1408 interior points. This problem is solved in (Tsai et al., 2010) using the golden section search algorithm for finding a good shape parameter. In (Esmailbeigi & Hosseini, 2014), authors solved the same problem using a genetic algorithm in the extended square  $[0; 1] \times [0; 1]$ . Here, we solve the considered problem using three different strategies for choosing the optimal shape parameter, the global shape parameter, the random variable shape parameter, and the variable shape parameter using PSO presented in this work.



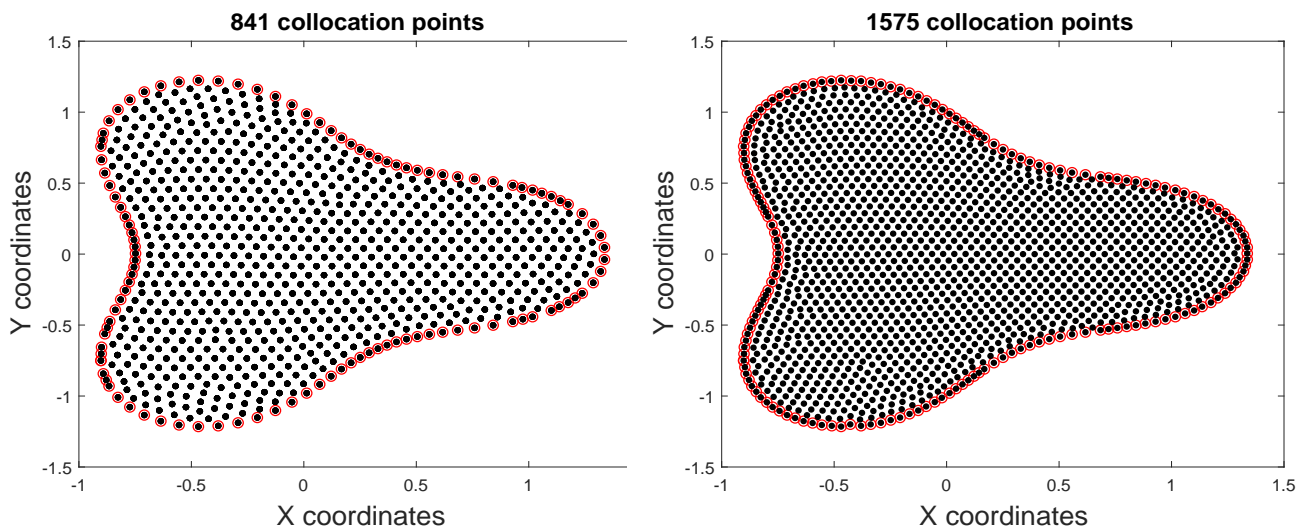


Figure 8. The collocation points in the computational domain with 841 points (left) and 1575 points (right) for the Helmholtz problem (39)

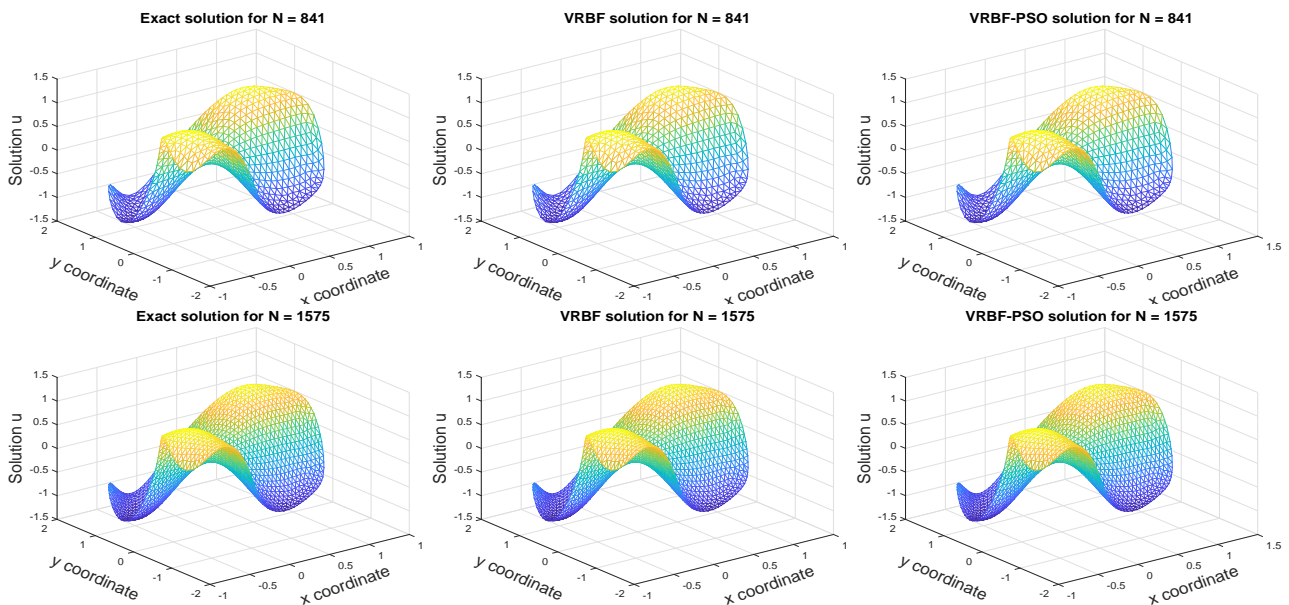


Figure 9. Results for the Helmholtz problem (39) at a different number of collocation points using the exact solution (first column), VRBF strategy (second column), and VRBF-PSO strategy (third column)

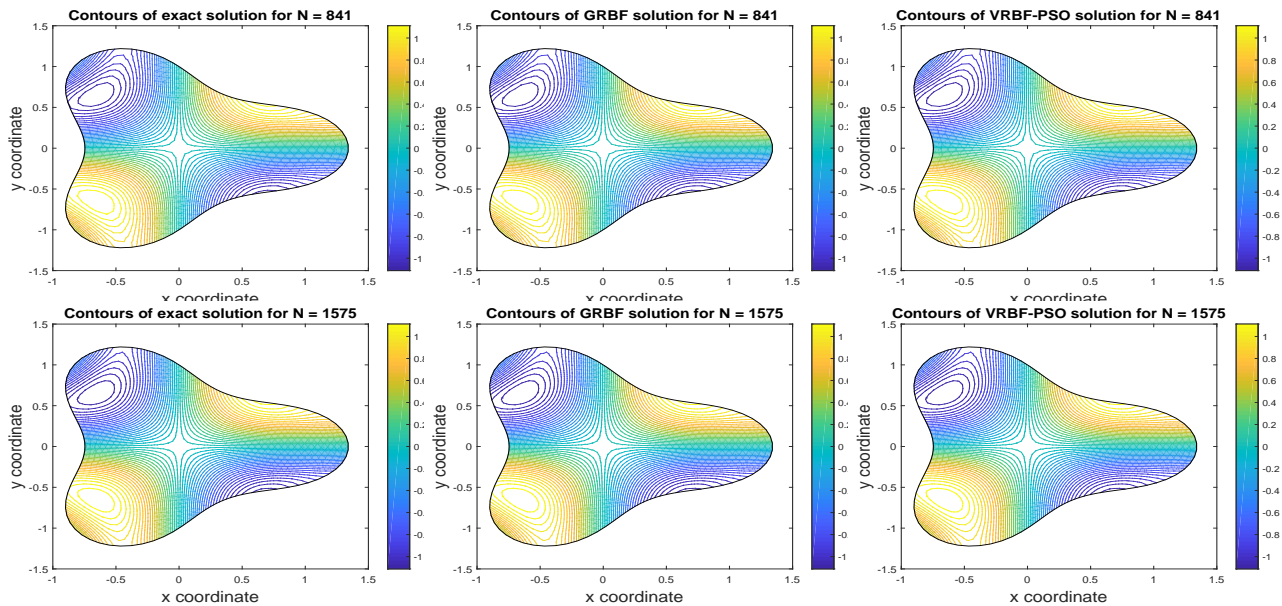


Figure 10. Contourlines for the Helmholtz problem (39) at a different number of collocation points using the exact solution (first column), GRBF strategy (second column), and VRBF-PSO strategy (third column)

Figure 9 illustrates the exact solutions and the obtained solutions using the variable shape parameters strategy in both applications, the no-use, and the use of PSO techniques using the two sets of collocation points respectively. In Figure 10, we plot 50 equidistributed contours of the corresponding results of the exact solution and numerical results from the GRBF strategy, and the VRBF-PSO strategy. It is apparent that the solution structures are in positive agreement with those published in (Tsai et al., 2010). In addition, the obtained results are compared with the published results in (Tsai et al., 2010; Esmailbeigi & Hosseini, 2014); it can be seen that our RBF strategy accurately resolves the solution features, and the boundary layers seem to be localized in the correct exact solutions.

To further visualize the comparisons, we display, in Table 7, the RMS errors, condition numbers, and optimal shape parameters for GRBF, VRBF, and VRBF-PSO strategies in the two sets of collocation points. Comparing the obtained results using the considered methods, it is crystal clear that the presented strategy method produces accurate solutions for the considered problem. Our strategy method accurately approximates the numerical solution to this boundary value problem. The results shown below compare favorably with the published results in the literature for the Helmholtz boundary value problems, see for instance (Tsai et al., 2010).

Table 7. RMS errors, condition numbers, and mean of the optimal shape parameters for the Helmholtz problem (39) in the two sets of collocation points using different optimal shape parameters strategies

| N    |               | GRBF       | VRBF       | VRBF-PSO   |
|------|---------------|------------|------------|------------|
| 841  | RMS error     | 4.7757E-06 | 3.0438E-04 | 1.1732E-05 |
|      | Cond. number  | 2.4192E17  | 2.1305E14  | 3.4850E20  |
|      | optimal shape | 1.765900   | 3.600100   | 5.545500   |
| 1575 | RMS error     | 2.2944E-07 | 7.9708E-06 | 1.0574E-07 |
|      | Cond. number  | 3.5172E18  | 5.0143E14  | 1.4811E20  |
|      | optimal shape | 2.065800   | 4.226500   | 6.870400   |

### 3.2.3 Convection-diffusion Problem

In this example, we consider the classical two-dimensional test problem defined by the equation (Tsai et al., 2010; Esmailbeigi & Hosseini, 2014):



$$\begin{aligned} \nabla^2 u(x, y) - (x^2 + y^2)u(x, y) - y \cos(y) \frac{\partial u}{\partial x} + \sinh(x) \frac{\partial u}{\partial y} &= f(x, y), \quad (x, y) \in \Omega, \\ u(x, y) &= g(x, y), \quad (x, y) \in \partial\Omega, \end{aligned} \quad (44)$$

where  $\Omega$  is a domain such that the boundary of which is a star-shaped region defined by the parametric equation (Tsai et al., 2010):

$$\partial\Omega = \{(x, y) \in \mathbb{R}^2 : x = (1 + \cos^2(4\theta)) \cos \theta, y = (1 + \cos^2(4\theta)) \sin \theta, -\pi \leq \theta \leq \pi\}. \quad (45)$$

The second member function  $f(x, y)$  and the boundary condition  $g(x, y)$  are generated from the exact solution

$$u(x, y) = \sin(\pi x) \cosh(y) - \cos(\pi x) \sinh(y). \quad (46)$$

The problem is solved using two sets of collocation points depicted in Figure 11. The domain from the left contains 200 boundary gridpoints and 213 interior collocation points, while the domain on the right is composed of 308 boundary gridpoints and 1630 interior gridpoints.

Table 8. RMS errors, condition numbers, and mean of the optimal shape parameters for the convection-diffusion problem (44) in the two sets of collocation points using different optimal shape parameters strategies

| N    |               | GRBF       | VRBF       | VRBF-PSO   |
|------|---------------|------------|------------|------------|
| 413  | RMS error     | 5.8923E-07 | 2.0512E-05 | 1.0345E-06 |
|      | Cond. number  | 3.4192E16  | 3.2130E15  | 3.7532E19  |
|      | optimal shape | 1.765900   | 3.600100   | 5.545500   |
| 1938 | RMS error     | 3.2486E-07 | 6.7152E-06 | 1.0004E-07 |
|      | Cond. number  | 3.1284E17  | 4.0143E13  | 1.5742E19  |
|      | optimal shape | 2.012800   | 3.175300   | 5.870400   |

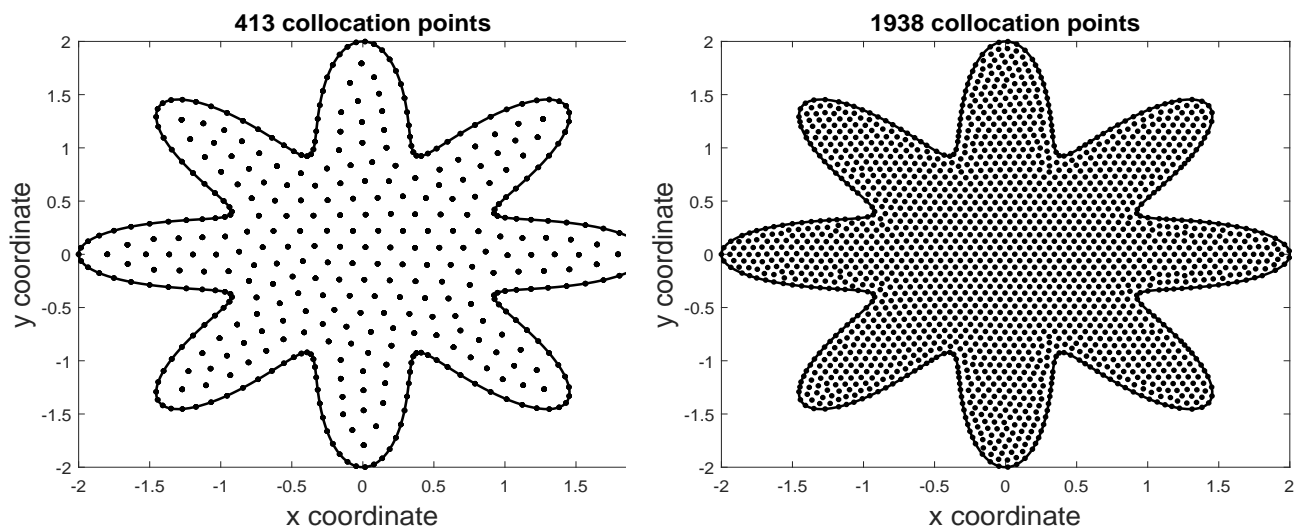


Figure 11. The collocation points in the computational domain with 413 points (left) and 1938 points (right) for the convection-diffusion problem (44)

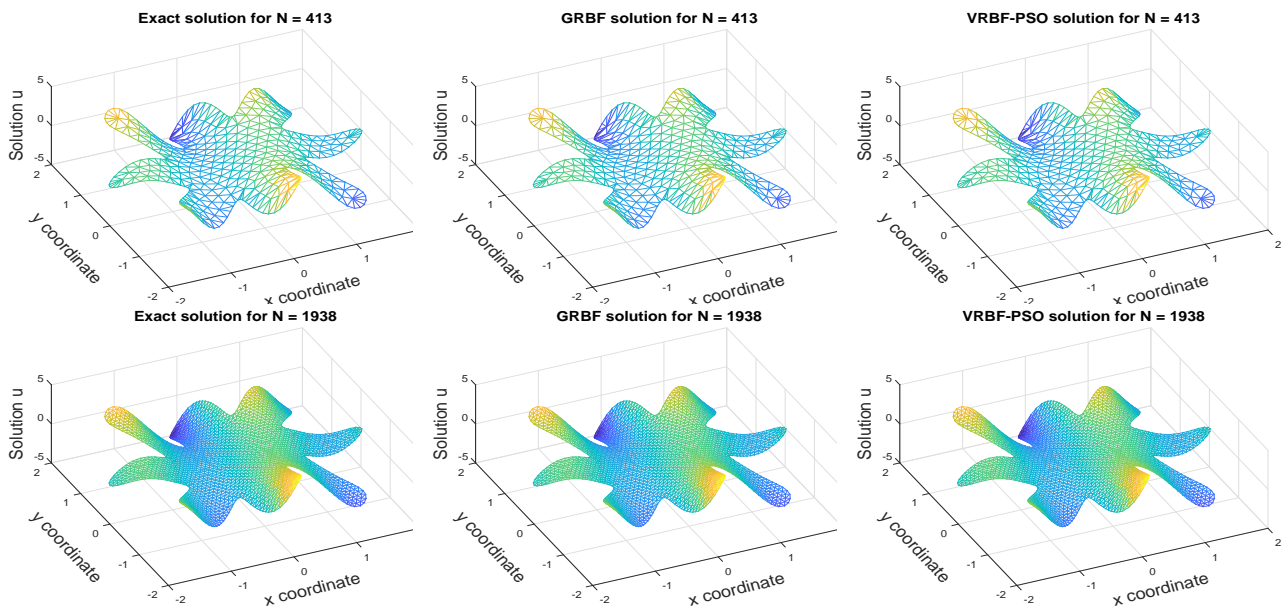


Figure 12. Results for the convection-diffusion problem (44) at a different number of collocation points using the exact solution (first column), GRBF strategy (second column), and VRBF-PSO strategy (third column)

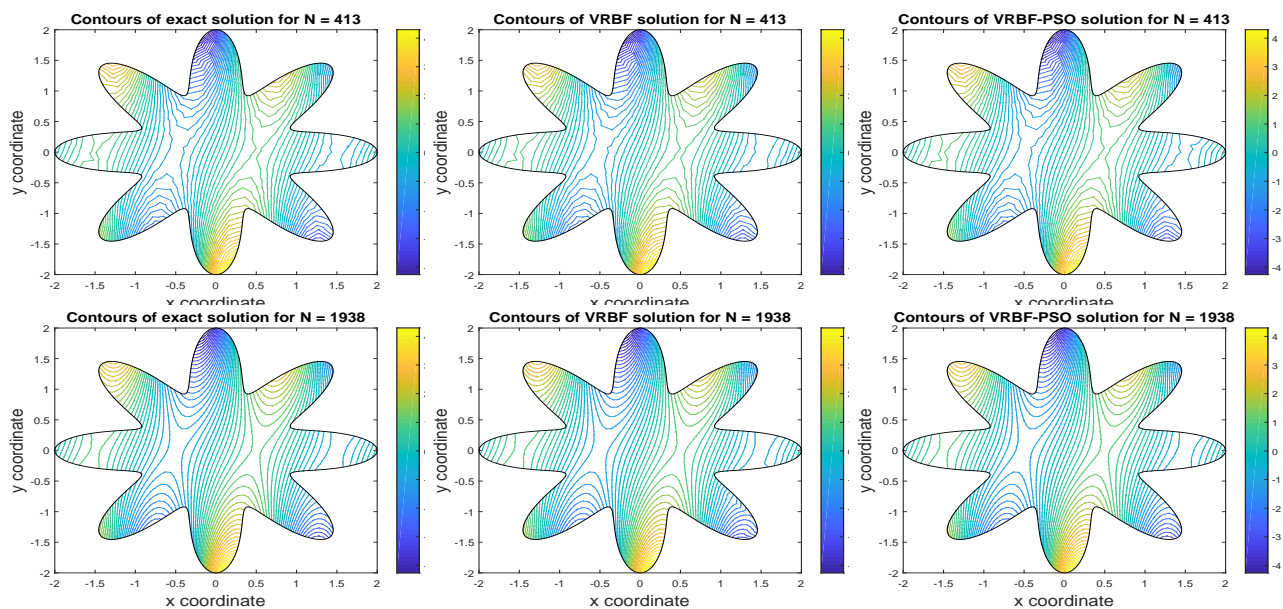


Figure 13. Contours for the convection-diffusion problem (44) at a different number of collocation points using the exact solution (first column), VRBF strategy (second column), and VRBF-PSO strategy (third column)

In Figure 12, we plot the exact solutions and the obtained solutions using the global shape parameters strategy without PSO techniques and the proposed strategy using the two sets of collocation points previously presented. In Figure 13, we report 50 equidistributed contours of the corresponding results of the exact solution and numerical results from the VRBF strategy without PSO and the VRBF-PSO strategy. The solution structures are in positive agreement with the published solutions (Tsai et al., 2010). In addition, the solution structures are also compared with the published results for example in (Tsai et al., 2010; Esmaeilbeigi & Hosseini, 2014); it can be seen that our RBF strategy resolves once more accurately the solution features and the boundary layers seem to be localized in the correct exact solutions.

To further visualize the comparisons, we display, in Table 8, the RMS errors, condition numbers, and optimal shape

parameters for GRBF, VRBF, and VRBF-PSO strategies in the two sets of collocation points. The proposed method produces accurate solutions for the considered problem. Our strategy method accurately approximates the numerical solution to this boundary value problem. The results shown (in Table 8) compare favorably with those obtained using other strategies for the convection-diffusion problem, for instance (Tsai et al., 2010).

### 3.2.4 Elliptic Equation With Variable Coefficients

The last two-dimensional boundary value problem in this work consists of an elliptic equation with variable coefficients and homogeneous Dirichlet boundary conditions, as stated by (Li et al., 2003):

$$\begin{aligned} \frac{\partial}{\partial x} \left( a(x, y) \frac{\partial}{\partial x} u(x, y) \right) + \frac{\partial}{\partial y} \left( b(x, y) \frac{\partial}{\partial y} u(x, y) \right) &= f(x, y), \quad (x, y) \in \Omega \\ u(x, y) &= g(x, y), \quad (x, y) \in \partial\Omega \end{aligned} \quad (47)$$

where the variable coefficients are assumed to be

$$a(x, y) = 2 - x^2 - y^2 \quad \text{and} \quad b(x, y) = e^{x-y}, \quad (48)$$

and the functions  $f(x, y)$  and  $g(x, y)$  are taken according to the exact solution defined by

$$u(x, y) = \exp \left( (x - 0.5)^2 - (y - 0.5)^2 \right). \quad (49)$$

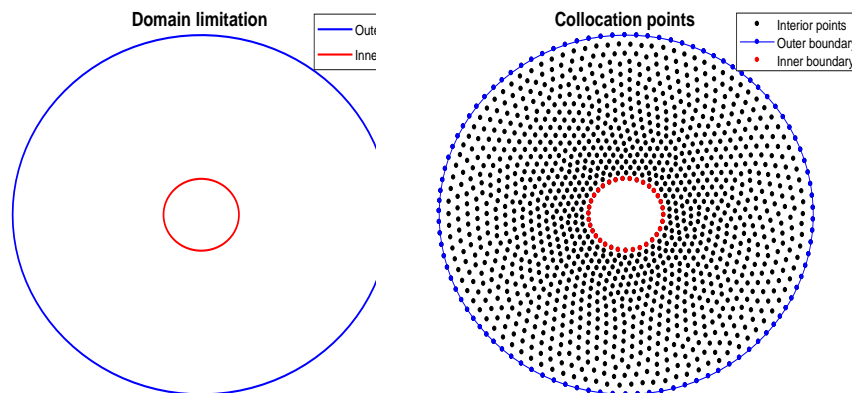


Figure 14. Domain limitation (left) and associated interior and boundary collocation points(right) for the problem (47)

This problem has been considered in (Koupaei et al., 2018) using the PSO strategy on choosing a global optimal shape parameter over the square  $[0; 1] \times [0; 1]$ . This strategy is selected in the present paper for comparison. In the current work, the elliptic equation (47) is defined in a circle of radius 0.5 with an internal circular hole of radius 0.1; both circles are centered in  $(x_0, y_0) = (0.5, 0.5)$ . We use 1350 collocation points, of which 100 are outer boundary points, 35 are inner boundary points, and 1215 are interior collocation points. The domain limitation and the collocation points are depicted in Figure 14. It is worth noting that no special nodal distribution is needed on the interface (blue marked points in Figure 14) to deal with the boundary conditions in the computational domain. The purpose of this elliptic problem is to compare the obtained numerical results using our optimal shape parameter strategy with the computed results using the global and variable shape parameters without the PSO strategy.

In Figure 15, the computed solutions for each strategy of choosing optimal shape parameters are presented, while Figure 16 depicts 50 equidistributed contours of these numerical solutions. Again for this boundary value problem, obtained results using the present strategy are more accurate than the obtained results using the strategies without PSO. The overall solution features for this example are preserved with good boundary detection. The computed results verify the accuracy and stability properties of the proposed RBF method.

Table 9. RMS errors, condition numbers, and mean of the optimal shape parameters for the problem (47) for the different strategies on choosing the optimal shape parameters

| N    |               | GRBF       | VRBF       | VRBF-PSO   |
|------|---------------|------------|------------|------------|
| 1350 | RMS error     | 2.7057E-06 | 3.5734E-09 | 5.1340E-10 |
|      | Cond. number  | 9.0777E19  | 1.1294E21  | 1.9843E21  |
|      | Optimal shape | 4.8447     | 4.0305     | 3.4868     |

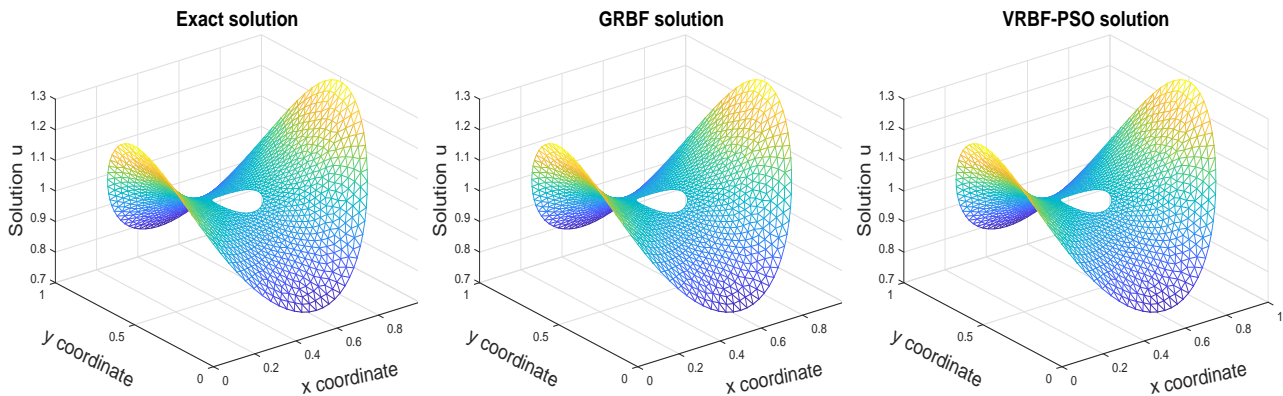


Figure 15. Mesh results for the elliptic problem (47) using the exact solution (first column), GRBF strategy (second column), and VRBF-PSO strategy (third column)

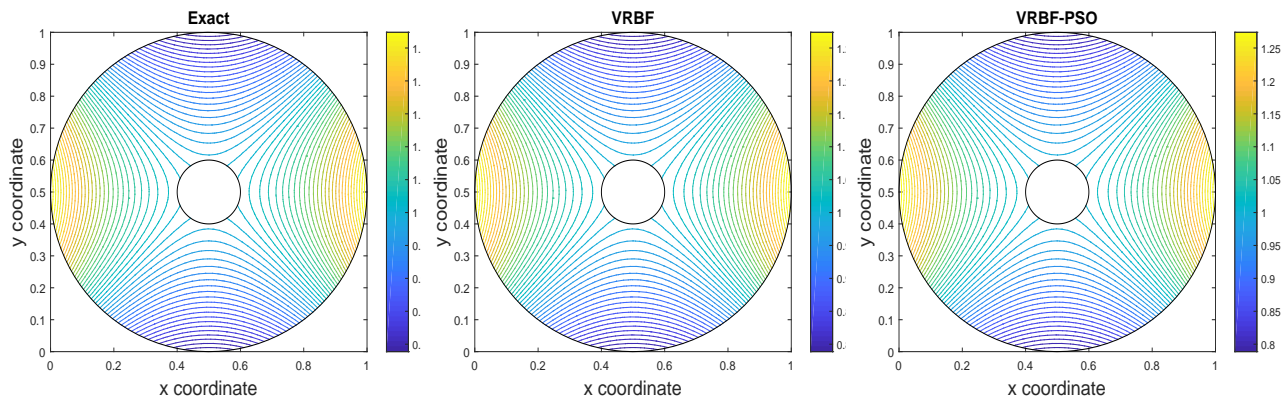


Figure 16. Contours plot results for the elliptic problem (47) using the exact solution (first column), VRBF strategy (second column), and VRBF-PSO strategy (third column)

For further comparisons, we summarize, in Table 9, the RMS errors, condition numbers, and optimal shape parameters for GRBF, VRBF, and VRBF-PSO strategies obtained in this test example. The presented strategy method produces accurate solutions even for the complex shaped domains in variable coefficient problems. Our strategy method accurately approximates the numerical solution to this boundary value problem. The results in table 9 compare favorably with the obtained results using other strategies for the elliptic problem; see for instance (Tsai et al., 2010; Koupaei et al., 2018).

In summary, the proposed strategy of choosing optimal variable shape parameters using the particle swarm optimization on solving boundary value problems produces satisfactory results for all the examples in the one and two-dimensional spaces. Furthermore, the obtained results for the considered test examples demonstrate the ability of the presented strategy to solve boundary value problems in complexly shaped domains.

#### 4. Concluding Remarks

We have presented a strategy for choosing an optimal set of variable shape parameters of Kansa's RBF scheme for numerical solutions to boundary value problems. The strategy uses a first stage of particle swarm optimization to determine

an optimal set of shape parameters by minimizing the modified RMS error. Subsequently, the acquired set of shape parameters is employed in the boundary value problem to compute an approximation of its solution. The proposed strategy is easy to implement and requires a few computational efforts to find a suitable set of variable shape parameters. In addition, from a practical viewpoint, the method is straightforward, irrespective of the smoothness of the complexly shaped domains under consideration.

The test functions are performed in the sense that the aim is to determine if the new algorithm is capable of obtaining results at least comparable to known results. Numerical results prove several examples of boundary value problems and positive expectations thoroughly. In light of the evidence, it is crystal clear that the performances of this presented approach are satisfactory. Findings highlight that using the proposed method (VRBF-PSO) is beneficial for computing partial differential equations in which the variable shape parameter with the local displacement in PSO provides a distinctive selection of the best solution. Moreover, the larger the number of collocations points is, the smaller the distance between two centers is; a fact that the proposed method may face numerical implementation difficulties and the higher the cost of time will be. The disadvantage of the proposed two-stages method is the need for more CPU time to computing the solution. The method is algorithmically complex but produces interesting results in terms of convergence and stability. For unsteady problems, this strategy may be more demanding regarding computational time.

In further work, the extension of this method in a multiobjective particle swarm optimization is to control the numerical errors of considered problems by maintaining the condition number of RBF matrices in lower bound to avoid ill-conditioned matrices. As the RBF matrices are hard to compute, adding control restrictions to the condition number and the numerical errors in the algorithm would reinforce the stability, convergence, and less CPU time to any real-life complex problems.

#### **Acknowledgements**

The authors would like to thank anonymous referees for giving very helpful comments and suggestions that have greatly improved this paper.

#### **Authors contributions**

Not applicable.

#### **Funding**

Not applicable.

#### **Competing interests**

The authors declare that they have no known competing financial interests or personal relationships that could have appeared to influence the work reported in this paper.

#### **Informed consent**

Obtained.

#### **Ethics approval**

The Publication Ethics Committee of the Canadian Center of Science and Education. The journal's policies adhere to the Core Practices established by the Committee on Publication Ethics (COPE).

#### **Provenance and peer review**

Not commissioned; externally double-blind peer reviewed.

#### **Data availability statement**

The data that support the findings of this study are available on request from the corresponding author. The data are not publicly available due to privacy or ethical restrictions.

#### **Data sharing statement**

No additional data are available.

#### **Open access**

This is an open-access article distributed under the terms and conditions of the Creative Commons Attribution license (<http://creativecommons.org/licenses/by/4.0/>).

#### **Copyrights**

Copyright for this article is retained by the author(s), with first publication rights granted to the journal.

## References

- Adewumi, A. O., Akindeinde, S. O., Aderogba, A. A., & Ogundare, B. S. (2020). A hybrid collocation method for solving highly nonlinear boundary value problems. *Heliyon*, 6(3), e03553. <https://doi.org/10.1016/j.heliyon.2020.e03553>
- Afiatdoust, F., & Esmaeilbeigi, M. (2015). Optimal variable shape parameters using genetic algorithm for radial basis function approximation. *Ain Shams Engineering Journal*, 6(2), 639-647. <https://doi.org/10.1016/j.asej.2014.10.019>
- Aiken, Q., Murray, A., & Lamichhane, A. (2022). Finding an effective shape parameter strategy to obtain the optimal shape parameter of the oscillatory radial basis function collocation in 3d. *Undergraduate Mathematics Day: Past Content*, 45(7), 1319. [https://ecommons.udayton.edu/mth\\_epumd/45](https://ecommons.udayton.edu/mth_epumd/45)
- Benaissa, B., Hocine, N. A., Khatir, S., Riahi, M. K., & Mirjalili, S. (2021). YUKI Algorithm and POD-RBF for Elastostatic and dynamic crack identification. *Journal of Computational Science*, 55, 101451. <https://doi.org/10.1016/j.jocs.2021.101451>
- Benaissa, B., Khatir, S., Jouini, M. S., & Riahi, M. K. (2023). Optimal Axial-Probe Design for Foucault-Current Tomography: A Global Optimization Approach Based on Linear Sampling Method. *Energies*, 16(5), 2448. <https://doi.org/10.3390/en16052448>
- Biazar, J., & Hosami, M. (2016). Selection of an Interval for Variable Shape Parameter in Approximation by Radial Basis Functions. *Advances in Numerical Analysis*. <https://doi.org/10.1155/2016/1397849>
- Buhmann, M. D. (2003). *Radial Basis Functions: Theory and Implementations*. Cambridge University Press. United Kingdom.
- Duan, J. S., Rach, R., & Wazwaz, A. M. (2013). Solution of the model of beam-type micro- and nano-scale electrostatic actuators by a new modified Adomian decomposition method for nonlinear boundary value problems. *International Journal of Non-Linear Mechanics*, 49, 159-169. <https://doi.org/10.1016/j.ijnlinmec.2012.10.003>
- Eberhart, R., & Kennedy, J. (1995). A new Optimizer using Particle Swarm Theory. In *MHS'95. Proceedings of the Sixth International Symposium on Micro Machine and Human Science*, 39-43. <https://doi.org/10.1109/MHS.1995.494215>
- Egorova, A. O., & Ye, K. K. (2020). Solution of inverse non-stationary boundary value problems of diffraction of plane pressure wave on convex surfaces based on analytical solution. *Journal of Applied Engineering Science*, 18(4), 676-680. <https://doi.org/10.5937/jaes0-28051>
- Elhani, D., Megherbi, A. C., Zitouni, A., Dornaika, F., Sbaa, S., & Taleb-Ahmed, A. (2023). Optimizing convolutional neural networks architecture using a modified particle swarm optimization for image classification. *Expert Systems with Applications*, 229, 120411. <https://doi.org/10.1016/j.eswa.2023.120411>
- Esmaeilbeigi, M., & Hosseini, M. M. (2014). A new Approach Based on the Genetic Algorithm for Finding a Good Shape Parameter in Solving Partial Differential Equations by Kansas Method. *Applied Mathematics and Computation*, 249, 419-428. <https://doi.org/10.1016/j.amc.2014.10.012>
- Fasshauer, G. E., & Zhang, J. (2007). On choosing "optimal" shape parameters for RBF approximation. *Numerical Algorithms*, 45, 345-368. <https://doi.org/10.1007/s11075-007-9072-8>
- Franke, R. (1979a). A Critical Comparison of Some Methods for Interpolation of Scattered Data. *Technical Report NPS-53-79-03*, Naval Postgraduate School. Monterey, CA
- Franke, R. (1979b). Scattered data interpolation: tests of some methods. *Math. Comput.*, 48, 181-200. <https://doi.org/10.2307/2007474>
- Fornberg, B., & Zuev, J. (2007). The Runge phenomenon and spatially variable shape parameters in RBF interpolation. *Computers & Mathematics with Applications*, 54(3), 379-398. <https://doi.org/10.1016/j.camwa.2007.01.028>
- Golberg, M. A., Chen, C. S. (1994). The theory of radial basis function applied to the BEM for inhomogeneous partial differential equations. *Boundary element communications*, 5, 57-61.
- Halassi, A. (2017). An Attractor-Based Multiobjective Particle Swarm Optimization. *International Journal of Applied and Computational Mathematics*, 3(2), 1019-1036. <https://doi.org/10.1007/s40819-016-0156-9>
- Halassi Bacar, A., & Rawhoudine, S. C. (2021). An attractors-based particle swarm optimization for multiobjective capacitated vehicle routing problem. *RAIRO - Operations Research*, 55(5), 2599-2614. <https://doi.org/10.1051/ro/2021119>
- Hardy, R. L. (1971). Multiquadric equations of topography and other irregular surfaces. *J. Geophysical Research*, 76(8), 1905-1915. <https://doi.org/10.1029/JB076i008p01905>



- Henderson, J., & Luca, R. (2016). *Boundary Value Problems for Systems of Differential, Difference and Fractional Equations*. Elsevier.
- Hon, Y. C., & Schaback, R. (2001). On unsymmetric collocation by radial basis functions. *Applied Mathematics and Computation*, 119(2-3), 177-186. [https://doi.org/10.1016/S0096-3003\(99\)00255-6](https://doi.org/10.1016/S0096-3003(99)00255-6)
- Irfan Shirazi, M., Khatir, S., Benaissa, B., Mirjalili, S., & Abdel Wahab, M. (2023). Damage assessment in laminated composite plates using modal Strain Energy and YUKI-ANN algorithm. *Composite Structure*, 303, 116272. <https://doi.org/10.1016/j.compstruct.2022.116272>
- Kansa, E. J., Aldredge, R. C., & Ling, L. (2009). Numerical simulation of two-dimensional combustion using mesh-free methods. *Engineering analysis with boundary elements*, 33, 940-950. <https://doi.org/10.1016/j.enganabound.2009.02.008>
- Kansa, E. J., Power, H., Fasshauer, G. E., & Ling, L. (2004). A volumetric integral radial basis function method for time-dependent partial differential equations I. Formulation. *Engineering Analysis with Boundary Elements*, 28, 1191-1206. <https://doi.org/10.1016/j.enganabound.2004.01.004>
- Kennedy, J., & Eberhart, R. (1995). Particle Swarm optimization. In *Proceedings of the Fourth IEEE International Conference on Neural Networks*, 4, 1942-1948. <https://doi.org/10.1109/ICNN.1995.488968>
- Koupaei, J. A., Firouznia, M., & Mahdi Hosseini, S. M. (2018). Finding a good shape parameter of RBF to solve PDEs based on the particle swarm optimization algorithm. *Alexandria Engineering Journal*, 57(4), 3641-3652. <https://doi.org/10.1016/j.aej.2017.11.024>
- Kumar, L., Pandey, M., & Ahirwal, M. K. (2023). Parallel Global Best-Worst Particle Swarm Optimization Algorithm for solving optimization problems. *Applied Soft Computing*, 142, 110329. <https://doi.org/10.1016/j.asoc.2023.110329>
- Leung, M. F., Ng, S. C., Cheung, C. C., & Lui, A. K. (2014). A new strategy for finding good local guides in MOPSO. In *2014 IEEE Congress on Evolutionary Computation (CEC)*, 1990-1997. <https://doi.org/10.1109/CEC.2014.6900449>
- Li, J., Cheng, A. H. D., & Chen, C., S. (2003). A comparison of efficiency and error convergence of multi-quadric collocation method and finite element method. *Eng. Anal. Boundary Elem.*, 27(3), 251-257. [https://doi.org/10.1016/S0955-7997\(02\)00081-4](https://doi.org/10.1016/S0955-7997(02)00081-4)
- Mehta, S., Agarwal, P., Shrivastava, P., & Barlawala, J. (2022). Differential bond energy algorithm for optimal vertical fragmentation of distributed databases. *Journal of King Saud University - Computer and Information Sciences*, 34(1), 1466-1471. <https://doi.org/10.1016/j.jksuci.2018.09.020>
- Micchelli, C. A. (1986). Interpolation of scattered data: distance matrices and conditionally positive definite functions. *Constructive approximation*, 1, 11-22.
- Kansa, E. J., Aldredge, R. C., & Ling, L. (2009). Numerical simulation of two-dimensional combustion using mesh-free methods. *Engineering analysis with boundary elements*, 33, 940-950.
- Powell, M. J. D. (1992). The theory of radial basis function approximation in 1990, in advances in numerical analysis. *Wavelets, subdivision algorithms and radial functions*, 2, 105-210. <https://doi.org/10.1093/oso/9780198534396.003.0003>
- Sarra, S. A., & Sturgill, D. (2009). A random variable shape parameter strategy for radial basis function approximation methods. *Engineering Analysis with Boundary Elements*, 33(11), 1239-1245. <https://doi.org/10.1016/j.enganabound.2009.07.003>
- Siraj-ul-Islam, Aziz, I., & Sarler, B. (2010). The numerical solution of second-order boundary-value problems by collocation method with the Haar wavelets. *Mathematical and Computer Modelling*, 52, 1577-1590. <https://doi.org/10.1016/j.mcm.2010.06.023>
- Skala, V., Karim, S. A. A., & Zabran, M. (2020). Radial basis function approximation optimal shape parameters estimation. In V. V. Krzhizhanovskaya, G. Zavodszky, M. H. Lees, J. J. Dongarra, P. M. A. Sloot, S. Brissos, & J. Teixeira (Eds.), *Computational science iccs 2020* (pp. 309317). Springer International Publishing.
- Slimani, M., Khatir, T., Boutchicha, D., Tiachacht, S., & Benaissa, B. (2022). Experimental sensitivity analysis of sensor placement based on virtual springs and damage quantification in CFRP composite. *Journal of Materials and Engineering Structures*, 9, 207-220.
- Sun, J., Wang, L., & Gong, D. (2023). A joint optimization algorithm based on the optimal shape parameter gaussian radial basis function surrogate model and its application. *Mathematics*, 11(14), 3169. <https://doi.org/10.3390/math11143169>
- Tansui, D., & Thammano, A. (2016). Sea Turtle Foraging Algorithm for Continuous Optimization Problems. in *Proceedings of 2016 6th International Workshop on Computer Science and Engineering*, 678-681.

- Tansui, D., & Thammano, A. (2020). Hybrid Nature-Inspired Optimization Algorithm: Hydrozoan and Sea Turtle Foraging Algorithms for Solving Continuous Optimization Problems. *IEEE Access*, 8, 65780-65800. <https://doi.org/10.1109/ACCESS.2020.2984023>
- Tchomté, S. K., & gourgand, M. (2009). Particle swarm optimization : A study of particle displacement for solving continuous and combinatorial optimization problems. *International Journal of Production Economics*, 121, 57-67. <https://doi.org/10.1016/j.amc.2010.12.053>
- Tsai, C. H., Kolibal, J., & Li, M. (2010). The golden section search algorithm for finding a good shape parameter for meshless collocation methods. *Engineering Analysis with Boundary Elements*, 34(8), 738-746. <https://doi.org/10.1016/j.enganabound.2010.03.003>
- Wang, Y., & Yang, Y. (2010). Particle swarm with equilibrium strategy of selection for multi-objective optimization. *European Journal of Operational Research*, 200(1), 87-197. <https://doi.org/10.1016/j.ejor.2008.12.026>
- Wendland, H. (2005). *Scattered Data Approximation*. Cambridge university press. New York, NY.
- Xiang, S., Wang, K., Ai, Y., Sha, Y., & Shi, H. (2012). Trigonometric variable shape parameter and exponent strategy for generalized multiquadric radial basis function approximation. *Applied Mathematical Modelling*, 36(5), 1931-1938. <https://doi.org/10.1016/j.apm.2011.07.076>
- Yaghouti, M., & Ramezannezhad Azarboni, H. (2017). Determining optimal value of the shape parameter c in rbf for unequal distances topographical points by cross-validation algorithm. *Journal of Mathematical Modeling*, 5(1), 5360. <https://doi.org/10.22124/jmm.2017.2225>
- Zheng, S., Feng, R., & Huang, A. (2020). The optimal shape parameter for the least squares approximation based on the radial basis function. *Mathematics*, 8(11), 1923. <https://doi.org/10.3390/math8111923>